

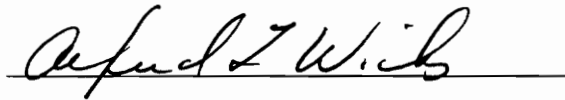
# Digital Frequency Demodulation for a Laser Vibrometer

by

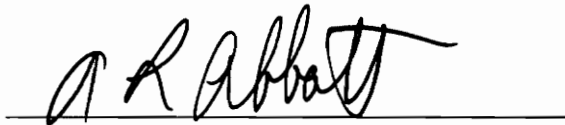
Christopher Joseph Cronin

Thesis submitted to the Faculty of the  
Virginia Polytechnic Institute and State University  
in partial fulfillment of the requirements for the degree of  
MASTER OF SCIENCE  
in  
Electrical Engineering

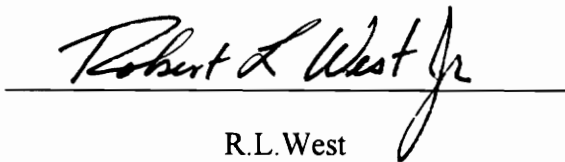
APPROVED:



A.L. Wicks, Co-Chairman



A.L. Abbott, Co-Chairman



R.L. West

May 1994  
Blacksburg, VA

C.2

LD  
5655  
V855  
1994  
C766  
C.2

# DIGITAL FM DEMODULATION FOR A LASER VIBROMETER

by

Christopher Joseph Cronin

Committee Co-Chair: A. L. Wicks  
Mechanical Engineering

Committee Co-Chair: A. L. Abbott  
Electrical Engineering

(ABSTRACT)

This thesis presents the design and simulation of a digital frequency demodulator applied to a Michelson interferometer-based scanning laser vibrometer. The laser vibrometer is a velocity transducer that produces frequency modulated signals that have traditionally been optically or electronically frequency shifted from baseband to an intermediate frequency. This shifting produces a narrow band modulation that may be demodulated with standard analog frequency demodulators. This thesis proposes replacing these traditional optics or electronic circuits with a digital frequency demodulator. The optics of a laser vibrometer can be constructed such that a near-perfect baseband quadrature representation is available for the frequency modulation. It will be seen that this representation is well suited for use by a digital frequency demodulator. This thesis applies the arctangent-type digital frequency demodulator to a laser vibrometer and demonstrates its superiority over other digital demodulation techniques. In addition some specialized signal processing to handle the special case of sine-dwell vibration tests is presented.

## DEDICATION

This thesis is dedicated to my wife Julie, my child to be, and my family and friends.

## ACKNOWLEDGMENTS

First I want to thank my wife Julie for being understanding during late nights when I was still at work.

I would not be here without my family. Thank you all.

I would like to thank Zonic for providing the funds for my work, and the Mechanical Engineering Department of Virginia Tech for letting me rummage through their old computers for the rest of the required components.

I would also like to thank Dr. L. D. Mitchell, Dr. R. L. West and Dr. A. L. Abbott for their discussions and support throughout my thesis development.

Finally I would like to give special thanks to Dr. Al Wicks who made sure that I made it into and out of the MS program, even though I'm a EE.

## TABLE OF CONTENTS

1. Introduction	1
2. Literature Review	5
3. Laser Vibrometer Techniques	10
3.1. Interferometers.....	10
3.2. Bragg Cell interferometer .....	14
3.3. Michelson Interferometer .....	15
4. Angle Modulation	17
4.1. Angle Modulation .....	17
4.2. Phase Modulation.....	17
4.3. Frequency Modulation.....	19
4.4. Relationship Between Phase and Frequency Modulation .....	20
5. Vibrometer Modulation Simulations	22
5.1. Target Velocity Parameters .....	22
5.2. Doppler Signal Parameters .....	22
5.3. Phase or Frequency Demodulation.....	23
5.4. Carrier To Noise Ratio Requirements .....	24
5.5. Real-Time Operation .....	25
5.6. Doppler Signal Simulation.....	25
6. Analog Frequency Demodulation	28
6.1. Envelope Detector for Frequency Demodulation .....	28
6.2. Zero-Crossings for Frequency Demodulation.....	30
6.3. Phase Locked Loop for Frequency Demodulation.....	31
7. Digital Frequency Demodulation	33

7.1. Why Digital Demodulation?.....	33
7.2. Comparison Methods .....	34
7.3. Arctangent-Type Digital Frequency Demodulation .....	35
7.4. Zero-Crossing Frequency Demodulator .....	43
7.5. Balanced Quadricorrelator Frequency Demodulator.....	44
7.6. Demodulator Selection for the Laser Vibrometer .....	46
8. Arctangent-type Demodulator Implementation Issues .....	49
8.1. Sampling Requirements .....	49
8.2. Phase Demodulator .....	50
8.3. Phase Unwrapping (overflow).....	50
8.4. Differentiation .....	51
9. Post-Demodulation Velocity Tracking .....	53
9.1. Proposed Configuration.....	53
9.2. Quadrature Detector LPF Design .....	58
9.3. CNR Dropout Detection .....	62
9.4. Magnitude of Doppler Quality Signal.....	63
9.5. Sum of Doppler Absolute Values Quality Signal.....	65
9.6. Application of the Sine-Dwell demodulator .....	66
10. Discussion of Results .....	70
11. Conclusion .....	73
12. Bibliography .....	75
13. Vita .....	76

# 1. Introduction

The laser vibrometer is a velocity transducer intended for non-contact vibration measurement. A typical setup for a laser vibrometer is shown in Figure 1. Laser vibrometers work on the Doppler principle by reflecting a laser beam off of a target object and looking at the optical frequency of the returned beam which has

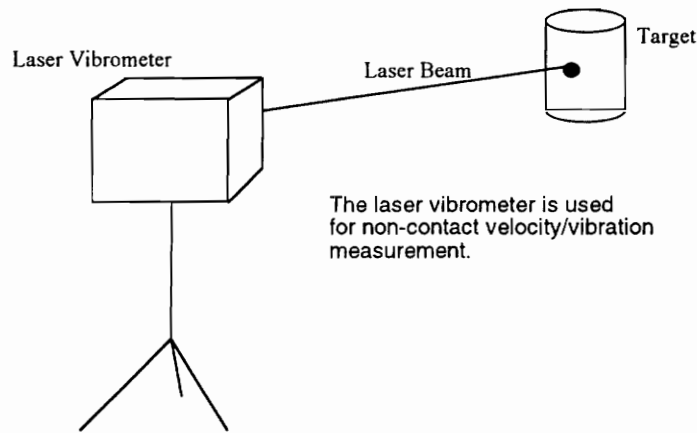


Figure 1. Typical vibration measurement test setup.

been Doppler shifted by the target. The reflected beam contains the frequency modulated velocity of the target object at an optical carrier frequency of the original beam's optical frequency. The reflected beam is then mixed with the original laser beam to remove the optical carrier. This results in a baseband frequency modulation which is converted to electrical signals via electro-optic sensors.

Frequency modulation is usually implemented as a narrow band modulation where the peak frequency deviation of the modulated signal from the carrier is small



compared to the frequency of the carrier. In the case of the laser vibrometer, where the carrier is zero, the modulation is infinitely wideband. For this reason standard analog frequency demodulators will not work directly on the signals provided by the laser vibrometer. To overcome this limitation laser vibrometer designers have chosen to convert the baseband frequency modulation to some non-zero carrier and then to apply one of the standard analog frequency demodulators. The conversion to a non-zero carrier is performed using one of two methods. Before describing these methods it is important to note that in addition to the baseband signal problem designers must cope with a return beam signal strength that varies greatly due to random effects such as target object surface texture. This large multiplicative noise problem is balanced by very little additive noise.

The first method to overcome the baseband signal problem optically shifts either the reference beam or the return beam in frequency so that when the two beams are mixed there remains a carrier at the optical shift frequency. After conversion to an electrical signal it is a standard narrow band frequency modulated signal. An analog frequency demodulator is then applied to extract the target object's velocity.

A second method to overcome the baseband signal problem generates a pair of quadrature frequency modulated signals at baseband, the Doppler signals. The quadrature Doppler signals are generated optically with a quarter-wave plate and are nearly perfect. These signals are then electronically frequency shifted to some intermediate frequency with a balanced modulator. As in the optical frequency shifting method an analog frequency demodulator is then applied to extract the target object's velocity.

Each of the above methods is a satisfactory method for extracting the velocity signals. However, it is interesting to see if the frequency demodulation may be performed without the need for electrical or optical frequency shifting. This requires a frequency demodulator to work on baseband signals. Traditional analog frequency demodulation techniques require a non-zero carrier, so they can not perform the baseband demodulation. Fortunately digital frequency demodulation techniques have been introduced that are able to work on baseband signals. Indeed the quadrature Doppler signals generated by a laser vibrometer with a quarter-waveplate are ideal for the digital demodulation techniques.

A standard analog technique for frequency demodulation, the zero-crossing method, is easily converted to a baseband digital implementation. This method measures the time between zero-crossings of the modulated signal to determine its frequency which is inversely proportional to the magnitude of the message signal. At baseband this method requires additional information to determine the sign of the message signal. Quadrature signals, generated easily by a laser vibrometer, provide the sign information in their lead/lag relationship. The zero-crossing method relies on accurate timing of the inter-zero-crossing period and is very susceptible to noise on the incoming signals.

A second digital frequency demodulation method, that also requires a pair of quadrature signals, determines the instantaneous phase of the demodulated signal with a four-quadrant arctangent function. The first derivative is then taken to complete the frequency demodulation. It will be shown that this method, the arctangent-type digital frequency demodulator or RE-TAN method, is optimum for the laser vibrometer. A great advantage of this method when applied to the laser

vibrometer is that the four-quadrant arctangent is immune to multiplicative noise which is significant in the laser vibrometer.

A third method, the balanced-quadricorrelator, combines the arctangent operation and first derivative operation of the arctangent-type demodulator into a single step by generating the first derivatives of the quadrature signals and then implementing the symbolic derivative of the four-quadrant arctangent function. The balanced quadricorrelator requires more computational power than the arctangent-type and it is not immune to multiplicative noise.

The next section of this thesis is a literature review describing recent contributions to the state of the art in the areas of frequency demodulation and laser vibrometry. Section three is a review of laser vibrometry which is a special case of laser velocimetry. Section four is an overview of angle modulation which includes phase and frequency modulation. Section five covers some standard techniques for analog frequency demodulation. The analog techniques then lead to the digital frequency demodulation techniques in section six. In reviewing the digital techniques extra attention is given to the required carrier-to-noise ratio (CNR) for each demodulation technique. Also in section six, one of the digital frequency demodulation techniques, the arctangent-type, is selected for the laser vibrometer. Following the selection of the arctangent-type demodulator, its implementation is considered in section seven. Section eight introduces a specialized demodulator for the sine-dwell vibration. Finally the results of the thesis are discussed and a conclusion is presented.

## 2. Literature Review

A laser vibrometer crosses the boundary between optics and electronics. Much work has been done on both parts. However the inherent qualities of the laser vibrometer's optics, particularly the capability of generating near-perfect quadrature signals, have not been matched to the electronics that exploit them best.

The fundamentals of laser doppler techniques including laser vibrometry are described in detail by Drain's text [1], which covers mostly laser velocimetry. Laser velocimeters measure the velocity of a target object by reflecting a laser beam off of the target and looking at the frequency shift of the reflected beam. This frequency shift is due to the Doppler effect and is thus linearly proportional to the velocity of the target object. A laser velocimeter is intended for a target that has some constant velocity component such as particles flowing in a liquid. The basic concept of velocimetry applies to laser vibrometry as well. A laser vibrometer is intended for a target that is vibrating but has a mean velocity of zero.

Analog angle modulation, which consists of phase and frequency modulation, is covered in many basic communications texts such as the those by Stremler and Couch [2,3]. In angle modulation either the phase or frequency of a carrier is linearly proportional to the message signal. The message signal is the signal that is to be transmitted. In the case of the laser vibrometer the velocity signal is the message signal. Most texts generally limit themselves to the narrow-band case of frequency modulation. This means that the peak frequency deviation from the carrier frequency is small compared to the carrier frequency. However the laser vibrometer generates a baseband frequency modulation which means there is no

carrier or that the carrier is 0Hz. With a peak deviation greater than zero and a carrier of zero the laser vibrometer's frequency modulation is infinitely wide-band. Therefore the discussions of frequency demodulation methods in the mentioned text's are used only to introduce the subject.

With the advent of high speed sampling and digital signal processing, digital frequency demodulation has become an alternative to analog frequency demodulation. Three digital methods will be discussed in this thesis: arctangent type, balanced quadricorrelator type, and zero-crossing type.

The first digital frequency demodulation method discussed here is the arctangent type also known as the RE-TAN or range-extended arctangent-type method described by Hagiwara and Nakagawa[4]. This method, after generating quadrature FM signals from the original signal, uses an arctangent function to determine the instantaneous phase of the message signal. A detailed description of each of the elements of the following equation is given in the section on angle modulation.

$$I(t) = \cos\left(\beta_f \int_{-\infty}^t m(x) dx\right)$$

$$Q(t) = -\sin\left(\beta_f \int_{-\infty}^t m(x) dx\right)$$

$$\theta(t) = \tan^{-1}\left(\frac{I(t)}{Q(t)}\right) = \beta_f \int_{-\infty}^t m(x) dx$$

where,

$I(t)$  = In - phase FM signal.

$Q(t)$  = Quadrature FM signal.

$m(t)$  = Message signal.

$\beta_f$  = FM constant.

[Eq. 1]

When applied to the laser vibrometer the first step, generating the quadrature signals, is unnecessary since the laser vibrometer generates near-perfect quadrature signals itself. The arctangent method then differentiates the signal and finally a phase unwrapping is performed to generate the fully frequency demodulated message signal. Minor modifications to the RE-TAN are made by Boutin and Kallel[5]. They show that by phase unwrapping before applying the difference function that the demodulator will work with a lower input carrier-to-noise ratio (CNR). A drawback of the RE-TAN method is that the phase unwrapping logic will overflow at some point in a real system.

The second digital frequency demodulation method discussed here is called the "quadrice correlator" or "balanced quadrice correlator" and is summarized by Boutin and Kallel. The balanced quadrice correlator performs the two steps of the RE-TAN method, the arctangent and the differentiation, in a single step by taking the first

derivatives of the two quadrature channels and implementing the symbolic derivative of the arctangent function.

$$m(t) = \frac{d}{dt} \left[ \tan^{-1} \left( \frac{Q(t)}{I(t)} \right) \right]$$

$$= \frac{I(t) \frac{dQ}{dT} - Q(t) \frac{dI}{dT}}{I^2(t) + Q^2(t)}$$

where,

[Eq. 2]

$I(t)$  = In - phase FM signal.

$Q(t)$  = Quadrature FM signal.

$m(t)$  = Message signal.

With the first difference function approximation of the first derivative the balanced quadricorrelator will generate a sinusoidal frequency-to-voltage characteristic not a linear one.

The third digital frequency demodulation method discussed here is the zero-crossing approach used by Zeng, Dominguez, and Wicks [6]. A signal's frequency is the inverse of its period and therefore the frequency of the signal is known if the period is known. The signal's period in turn may be measured by measuring the time between the signal's zero-crossings. If the signal is a frequency modulated signal at baseband then there is still a sign ambiguity after the magnitude of the message signal is obtained by determining the FM signal's frequency. If the signal is velocity, the speed is known but the direction is not. In order to determine the sign of the message signal some additional information is required such as a quadrature

representation where the sign is stored in the lead/lag relationship of the quadrature signals.

This thesis will apply these three digital demodulation methods to simulated laser vibrometer quadrature Doppler signals and determine which is most appropriate for a real-time implementation. The same communications texts [2,3] used to cover angle modulation also describe comparison methods such as the 'signal-to-noise ratio versus carrier-to-noise ratio' (SNR vs. CNR) test that will be used to compare the several digital demodulation methods reviewed in this thesis.

There have been other approaches to using digital techniques with laser interferometers. Oka, Mizuno, and Ohtsuka [7] use Fourier-transform techniques on an optical heterodyne system. This method will not be addressed further in this thesis as this thesis uses the quadrature Doppler signal laser vibrometer.

During the testing and implementation of the digital demodulation methods reviewed in this thesis some basic digital signal processing techniques are used. They include sampling and digital filtering. These techniques are described in many texts such as Jackson[8] or Oppenheim[9].



### 3. Laser Vibrometer Techniques

A laser vibrometer is a velocity transducer used for non-contact vibration measurement. With the addition of a scanning system the laser vibrometer is able to measure a structure's velocity at many points in a short time.

#### 3.1. Interferometers

The interferometer is a velocity transducer that determines a target's velocity by reflecting a laser beam off of the target. The Doppler effect causes the target-reflected light to have a slightly different frequency than the transmitted light. Drain derives this effect using various approaches[3]. The momentum approach is briefly reviewed here.

Light has wave-like properties and particle-like properties. Using the particle nature of light each photon emitted has a finite energy given by,

$$e = h\nu$$

where,

$e$  = photon energy

$h$  = Planck's constant

$\nu$  = frequency

[Eq. 3]

When the photon elastically collides with a moving target object, both the photon and the target object have a change in momentum. Figure 2 shows the laser source

S, the point of impact on the target P, the observer's location Q, and the velocity vector of the target V.

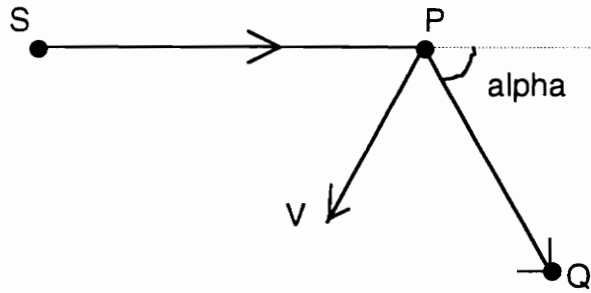


Figure 2. Diagram of doppler shift due to impact of a photon from source S with a target P with velocity V as seen by an observer at Q.

The change in momentum of the photon is given by,

$$\delta M = \frac{2h\nu}{c} \sin\left(\frac{\alpha}{2}\right)$$

where,

[Eq. 4]

$\delta M$  = change in photon momentum

$c$  = speed of light ( $3 \times 10^8 \text{ m/s}$ )

$\alpha$  = angle of impact

From this equation it is obvious that for the change in momentum to occur the frequency of the photon must change since the other components are constants.

The frequency shift is given by Drain [1] as,

$$\Delta\nu = \frac{2V_x}{\lambda}$$

where,

[Eq. 5]

$\Delta\nu$  = frequency shift of reflected laser beam

$V_x$  = target's velocity along the laser beam axis

$\lambda$  = wavelength of laser beam

Note that this difference in frequency is linearly proportional to the velocity of the target object.

Now that the frequency difference has been shown to be linearly proportional to the velocity of the target object, its usefulness will be addressed. From a signal communications point of view, everything is in place for a frequency demodulation except that the carrier, which is the transmitted beam, is in the visible electromagnetic spectrum rather than the usual radio frequency (RF) spectrum. The natural thing to do is to electronically mix the FM signal with a reference carrier to frequency shift it down to an intermediate frequency. If the reference carrier frequency is the same frequency as the modulation's carrier, then the resultant modulation is centered at 0Hz, it has no carrier, it is at baseband. The following subsections describe optical setups for methods that shift the carrier to an intermediate frequency and that shift the carrier to baseband.

Both methods for converting the optical frequency modulation to a standard narrow-band frequency modulation have a few things in common. Each method divides the source beam into two components. One is bounced off of the target which changes the reflected beam's frequency proportional to the target's velocity. The second beam, the reference beam, is kept within the vibrometer. The two beams are then combined and converted to electrical signals on a photodetector. Nonlinearities in the photodetector cause the 'mixing' of the two signals resulting in components at the sum of the two frequencies and at the difference of the two frequencies. The equation for the light intensity measured by the photodetectors is given by,

$$i(t) = B(E_1 \cos(2\pi\nu_1 + \theta_1) + E_2 \cos(2\pi\nu_2 + \theta_2))^2$$

$$i(t) = B\left(\frac{1}{2}(E_1^2 + E_2^2) + E_1 E_2 \cos(2\pi(\nu_1 - \nu_2)t + (\theta_1 - \theta_2))\right)$$

where,

$i(t)$  = Intensity of light on photodetector.

$B$  = Photodetector constant

$E_1, E_2$  = Amplitude of each mixed beam .

$\nu_1, \nu_2$  = Frequency of each mixed beam .

$\theta_1, \theta_2$  = Phase of each mixed beam .

[Eq. 6]

The sum frequency is at twice the original beam's optical frequency and is therefore irrelevant (the electrical circuits will filter it out even if the photo detectors do not). The difference frequency is in the normal radio frequency region or at

baseband and can be demodulated with electrical demodulators. The DC component may be removed with a high-pass filter (HPF).

### 3.2. Bragg Cell interferometer

The Bragg cell interferometer shown in Figure 3 uses a Bragg cell, which optically shifts a beam's optical frequency, on the reference beam (or the target beam) before recombination so that after recombination the velocity of the target object is frequency modulated at some non-zero carrier. The optical shift frequency becomes the carrier of the electrical frequency modulation. To extract the velocity of the target object one of the standard analog frequency demodulation techniques is used.

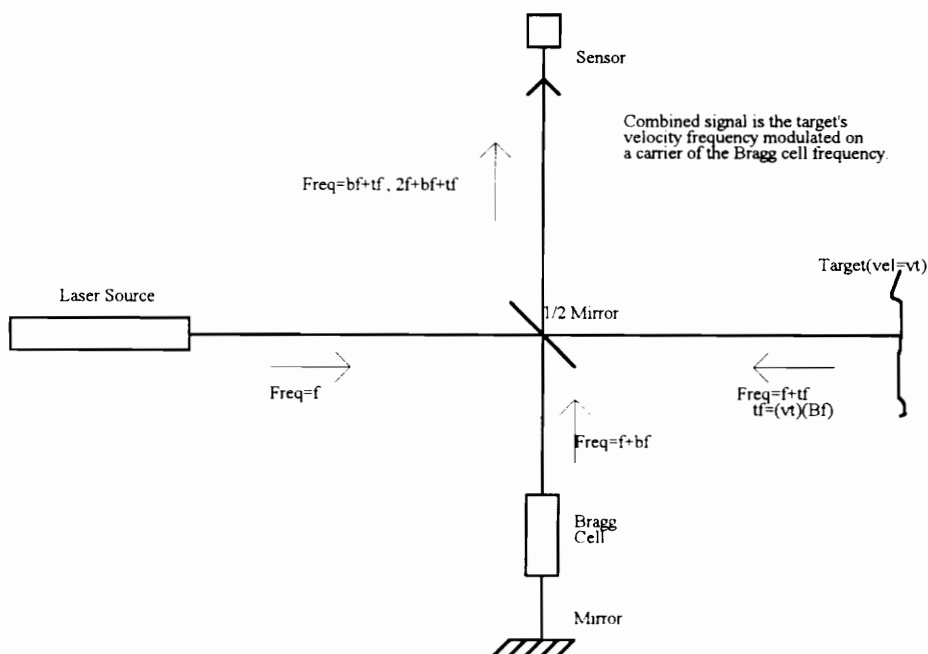


Figure 3. An example setup for an interferometer using a Bragg cell to optically shift the reference beam.

### 3.3. Michelson Interferometer

The basic Michelson interferometer with quadrature direction discrimination shown in Figure 4 generates two near perfect quadrature signals. The laser source beam is split into two beams: a reference beam which is reflected off of a local mirror, and a target beam which is reflected off of the target whose velocity is to be determined.

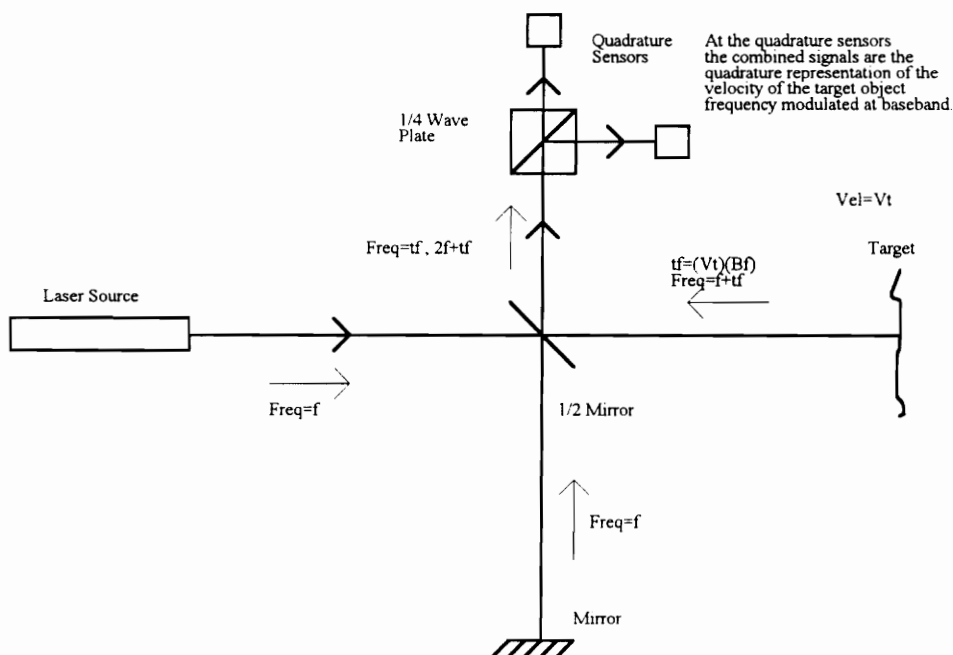


Figure 4. Michelson interferometer with quadrature direction discrimination.

The two beams are then combined and directed through a beam splitter which splits the combined beams into two beams with circular polarization, that is the polarizations are 90 degrees out of phase (perfect quadrature). The beams are

collected on separate collectors to produce a near-perfect electrical quadrature representation of the target object's velocity frequency modulated at baseband. These quadrature channels allow the direction of the target object's velocity to be determined. In addition, this paper shows how these baseband quadrature channels are perfect for the application of a digital frequency demodulator. Also if a standard analog frequency demodulation is desired then through electrical mixing a narrow-band frequency modulation similar to that produced by the Bragg cell setup can be produced from the quadrature baseband channels.

## **4. Angle Modulation**

In this section angle modulation is reviewed as it applies to the research done here, see such texts as Couch [3] for a more in-depth discussion. During the following section, the signal of interest that will be modulated then demodulated is called the message signal. In the laser vibrometer application, the message signal is the target object's velocity.

### **4.1. Angle Modulation**

Angle modulation includes both frequency and phase modulation. In both cases the phase of the modulated signal is related to the message signal. For phase modulation the phase of the modulated signal is linearly proportional to the message signal. For frequency modulation the frequency of the modulated signal is linearly proportional to the message signal and the phase is linearly proportional to the integral of the message signal.

### **4.2. Phase Modulation**

The modulated signal for phase modulation is,



$$g(t) = \cos(2\pi f_c t + \beta_p m(t))$$

where,

$\beta_p$  = phase modulation constant [rad / volt] [Eq. 7]

$m(t)$  = message signal [ volt ]

$f_c$  = carrier frequency [Hz]

The amplitude modulation does not contain any information about the message

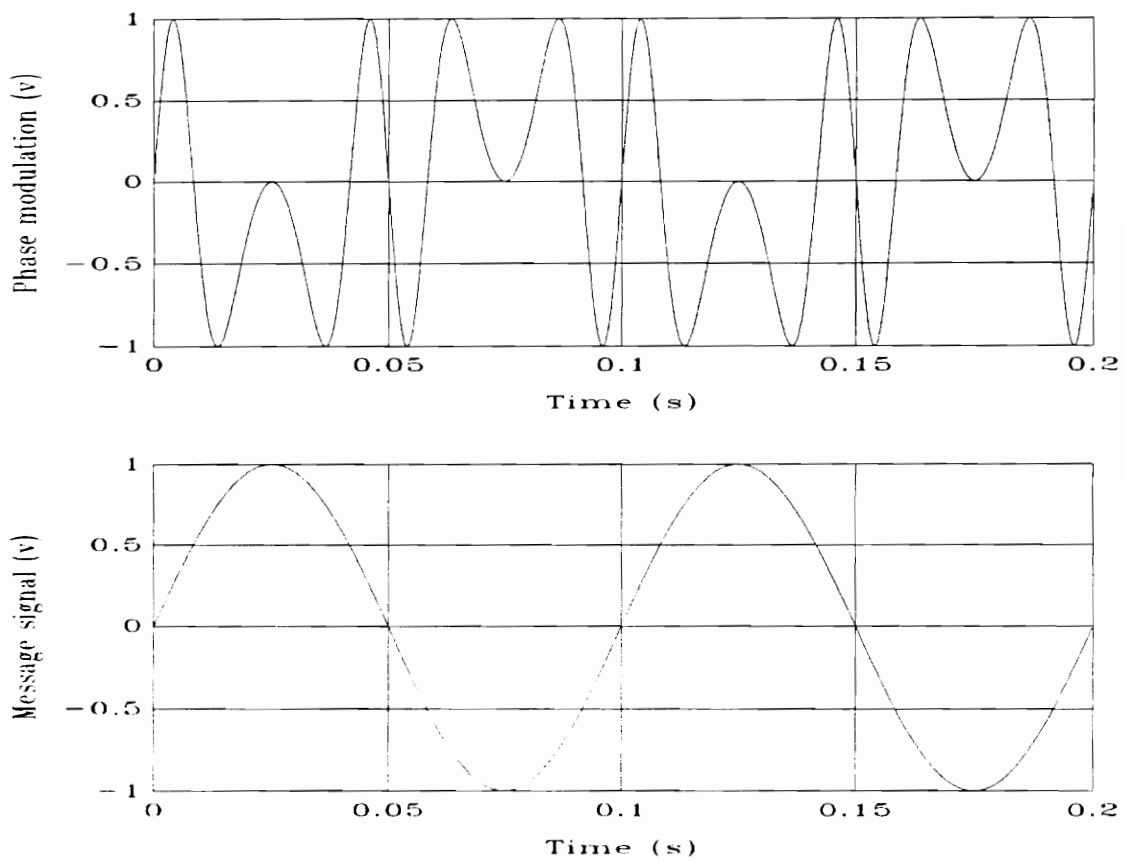


Figure 5. Phase modulation. ( $f_m$  = message frequency = 10 Hz,  $f_c$  = carrier frequency = 0 Hz,  $f_s$  = sampling frequency = 5 kHz,  $\beta_p$  = phase modulation constant =  $2\pi$ )

signal but it is shown as a function of time since it generally varies due to attenuation, gains, etc.. A benefit of phase modulation and frequency modulation is that the amplitude modulation is irrelevant so arbitrary gains in the system, such as multiplicative noise, will not add error. However additive noise will introduce error and a small amplitude of the modulated signal will aggravate an additive noise problem. An example of a phase modulation is given in Figure 5. This modulation is plotted at baseband with a phase modulation constant of  $2\pi$  to illustrate that the phase of unity-amplitude sinusoid is proportional to the message signal. In order to demodulate this baseband signal a quadrature detector would have to be used.

### 4.3. Frequency Modulation

The modulated signal for frequency modulation is,

$$g(t) = \cos\left(2\pi f_c t + \beta_f \int_{-\infty}^t m(x) dx\right)$$

$\beta_f$  = frequency modulation constant [rad / sec / volt] [Eq. 8]  
 $m(t)$  = message signal [volt]  
 $f_c$  = carrier frequency [Hz]

Here the frequency of the modulated signal is linearly proportional to the amplitude of the message signal. As in phase modulation, the amplitude modulation of the frequency modulated signal does not contain any information about the message signal. A frequency modulation is shown in Figure 6. It can be seen that the frequency is proportional to the message signal's magnitude. In this example the

carrier frequency is larger than the peak deviation due to the modulated signal; therefore, the modulated signal's frequency is always greater than zero.

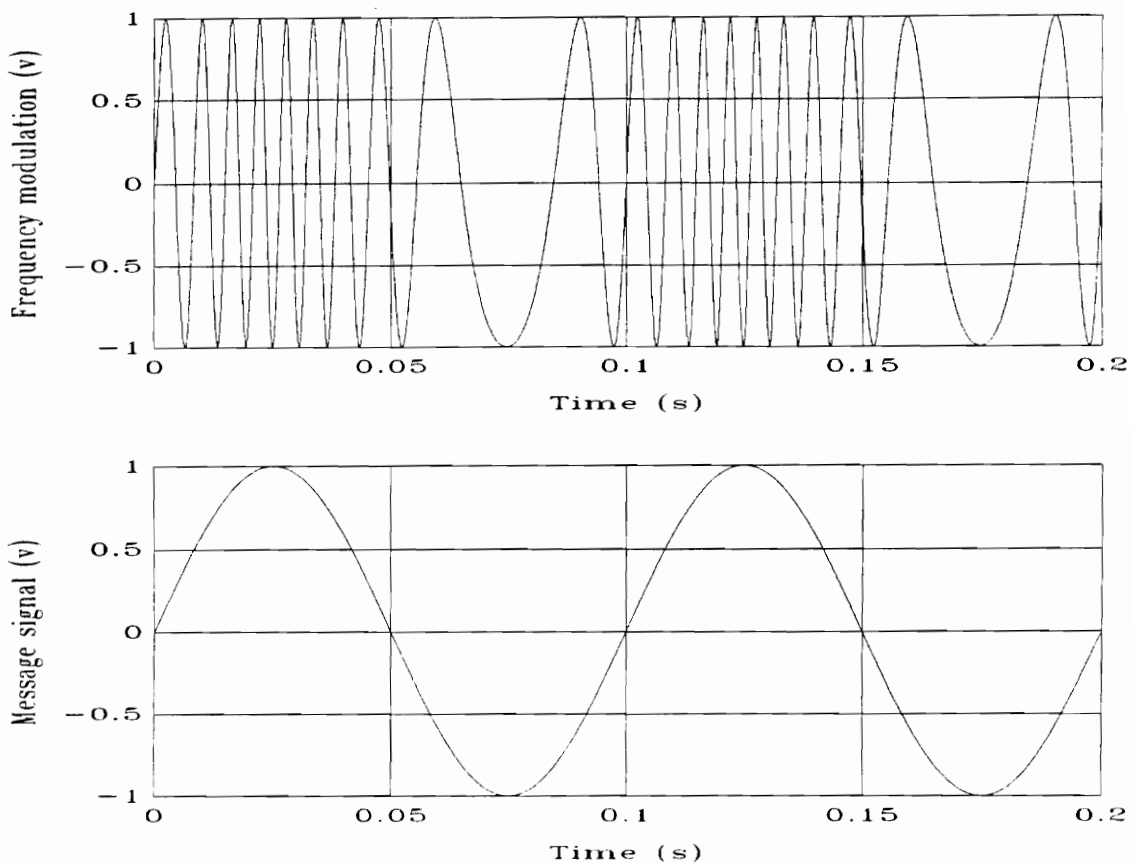


Figure 6. Frequency modulation.(fm = message frequency = 10 Hz, fc = carrier frequency = 100 Hz, beta = frequency modulation constant = 0.1 Hz/volt, fs = sampling frequency = 5 kHz).

#### 4.4. Relationship Between Phase and Frequency Modulation

Phase modulation and frequency modulation are related in that frequency modulation can be achieved by first integrating the message signal and phase

modulating the result. More importantly for this research, a frequency demodulation may be performed by following a phase demodulation with a differentiation operation (Figure 7). In a laser vibrometer the target object's velocity frequency modulates the return signal and it will be seen later that a digital phase demodulation is ideal for this system. To complete the frequency demodulation a differentiation operation is performed after the phase demodulation.

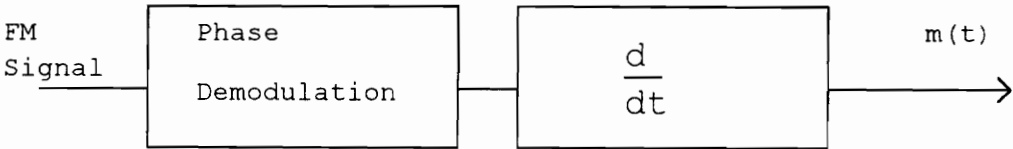


Figure 7: Frequency demodulation performed with a phase demodulator.

## 5. Vibrometer Modulation Simulations

With vibrometry and angle modulation reviewed, the frequency modulation generated by a He-Ne laser Michelson interferometer is simulated.

### 5.1. Target Velocity Parameters

For these simulations the target's velocity is assumed to be sinusoidal with an amplitude below 1m/s and a frequency below 30kHz. The sinusoidal specification simplifies the mathematics for frequency demodulation. In addition the test most frequently run with the laser vibrometer for which this paper is written is a sine-dwell test where a single known frequency is used. Furthermore the usual excuse that the generalization will hold fairly well if the maximum frequency of a multi-frequency signal is used in the stead of the single frequency used in these calculation still holds.

### 5.2. Doppler Signal Parameters

The Doppler signals generated by a Michelson interferometer have the usual frequency modulation parameters. The frequency modulation constant is determined by the laser light frequency. The bandwidth of the modulated signal is dependent on the frequency modulation constant and the maximum target object velocity that is specified.

To determine the frequency modulation constant the derivation of the doppler shift for the laser vibrometer is used again. Referring back to Equation 4

the 632nm wavelength He-Ne laser source and 1m/s target velocity are used to determine a maximum frequency shift and frequency modulation constant of,

$$v_{MAX} = \frac{2V_x}{\lambda} = \frac{2(1\frac{m}{s})}{632nm} = 3.16MHz$$

$$\beta_f = 3.16 \frac{MHz}{m/s}$$
[Eq. 9]

### 5.3. Phase or Frequency Demodulation

From the discussion of angle modulation it was seen that frequency modulation and phase modulation are closely linked. A frequency demodulation may be performed by performing a phase demodulation and then taking the first derivative of the result. Referring back to the physical process that the laser vibrometer measures, it can be seen that if the velocity is frequency modulated then a phase demodulation will produce the integral of the velocity: the relative position of the target object. It is important to recognize that it is the relative position of the target object, not the absolute position, that is measured. There is a phase ambiguity involved. The target is some unknown integral number of wavelengths plus some known fraction of a wavelength away from the vibrometer.

The importance of recognizing that a phase demodulation will generate a relative position signal is that the relative position signal is just as useful as the velocity signal in many instances. Particularly, this paper is written with an application in mind where the single sinusoidal velocity is fit to determine its magnitude and phase relative to some known signal of a known frequency. Since

the frequency is known the relative position signal can be fit just as easily and then the derivative of the fit signal is made, taken into account the factor of  $1/j\omega$ .

It will be seen in the following sections that the relative position signal will be much cleaner than the velocity signal. This is of course expected since the differentiation operation magnifies high frequency noise.

#### **5.4. Carrier To Noise Ratio Requirements**

The laser vibrometer bounces a source laser beam off of a target and then receives the reflected beam. This reflected beam suffers from attenuation due to path length, surface finish of the target, angle of incidence, and a finite receive aperture width. Viewing the aperture as being divided into many differential elements of 2D space, each element receives light from a slightly different target location and thus a slightly different path length. The different path lengths cause random phase accumulations resulting in constructive or destructive interference and a channel characteristic similar to traditional multipath-fading channels. This is aggravated by target texture. Indeed characterizing the channel is futile because the channel will be completely different if the target is changed, the angle of incidence onto the target is changed, or even if the laser vibrometer is moved a few centimeters towards or away from the target.

For this paper it is only important to realize that the channel will fade and that the best demodulator for the application will require a minimum input carrier-to-noise ratio. In addition complete 'dropouts' of the channel can not be avoided and the best demodulator will gracefully recover from an insufficient carrier-to-noise ratio.

## 5.5. Real-Time Operation

In order for a laser-vibrometer demodulator to be effective it must operate in real time or block-mode real time. If the demodulator is analog this is not a problem. However for digital systems this requires sampling and therefore processing at a minimum of 10MHz.

## 5.6. Doppler Signal Simulation

The laser doppler vibrometer return signals are essentially the velocity of the target object frequency modulated at baseband. The phase modulation constant for a laser vibrometer is

$$\beta_p = \frac{2\pi}{\lambda/2} \text{ rad / nm} \quad [\text{Eq. 10}]$$

$\lambda =$  wavelength of laser source (nm)



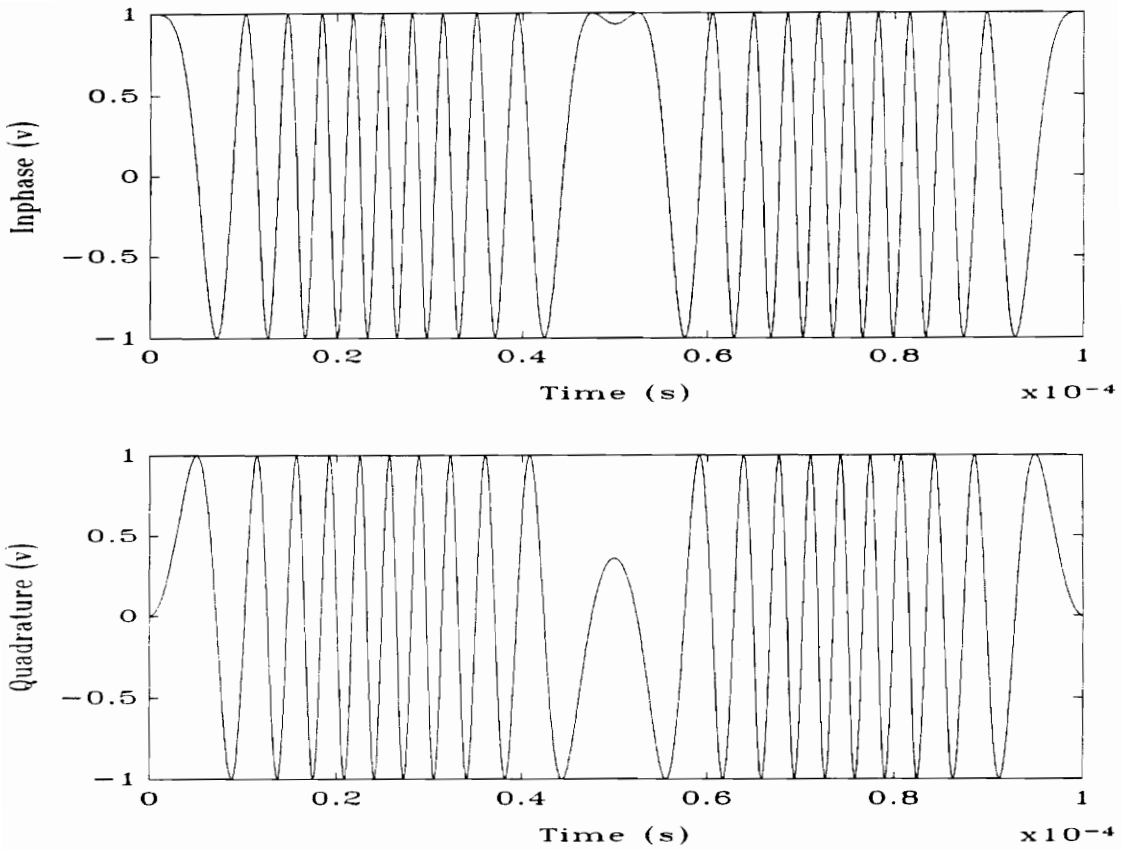


Figure 8.Doppler signal simulations.

For the case of a 632 nm laser source the phase modulation constant is 19.88 Mrad/m. This translates to 19.88 Mrad/(m/s) or 3.16 MHz/(m/s) for the frequency modulation constant. Simulated doppler signals for a laser vibrometer with quadrature signals are shown in Figure 8. Not shown in the figure is the amplitude modulation due to laser speckle. This amplitude modulation is important because it will greatly affect the carrier-to-noise ratio (CNR) of the Doppler signals. For this research it is only important to quantify the carrier-to-noise ratio required for a demodulation method to work. Therefore an additive white Gaussian noise is added

to the simulated Doppler signals which will be used to test the various frequency demodulation methods. To decrease CNR, either the amplitude of the Doppler signals can be changed or the level of the noise can be changed. Here the level of noise will be changed.. Plots of the Doppler signals with additive noise are shown in Figure 9. The simulations used in this thesis allow different amounts of additive noise in the Doppler signals.

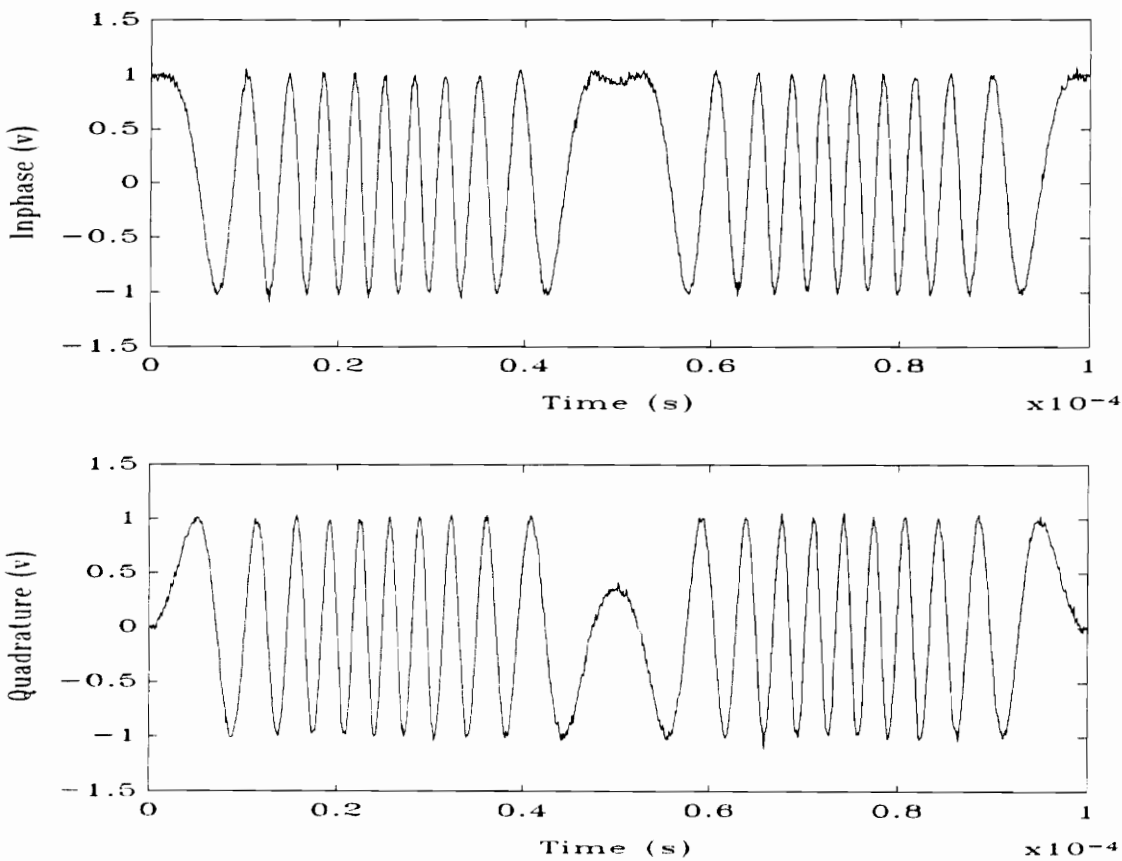


Figure 9. Doppler signals with additive noise.

## 6. Analog Frequency Demodulation

To frequency demodulate a signal, a method must be used that converts frequency to amplitude linearly. Some analog techniques to do this are presented in this section along with examples of how the method works. Standard analog techniques for frequency demodulation include envelope detectors and phase-locked loops. It will be seen that these techniques break down when the frequency modulation has no carrier.

### 6.1. Envelope Detector for Frequency Demodulation

Referring to Equation 8 and assuming that  $A(t)$  is a known constant or can be eliminated with limiters, a frequency modulated signal can be converted to an amplitude modulated signal simply by differentiating

$$\frac{d}{dt} \left\{ A \sin \left( 2\pi f_c t + \beta_f \int_{-\infty}^t m(x) dx \right) \right\} =$$
$$A(2\pi f_c + \beta_f m(t)) \cos \left( 2\pi f_c t + \beta_f \int_{-\infty}^t m(x) dx \right) \quad [\text{Eq. 11}]$$

The amplitude of this signal holds the information of the message signal and can be detected with standard amplitude demodulation techniques such as an envelope detector. The output of the envelope detector would be the absolute value of the derivative's amplitude,

$$o(t) = |A_2 \pi f_c + A \beta_f m(t)| \quad [\text{Eq. 12}]$$

Note that if the carrier frequency is not greater than the message signal amplitude times the modulation constant then some of the information in the signal will be lost. In the extreme case where there is no carrier, the output of the envelope detector will be the absolute value of the message signal.

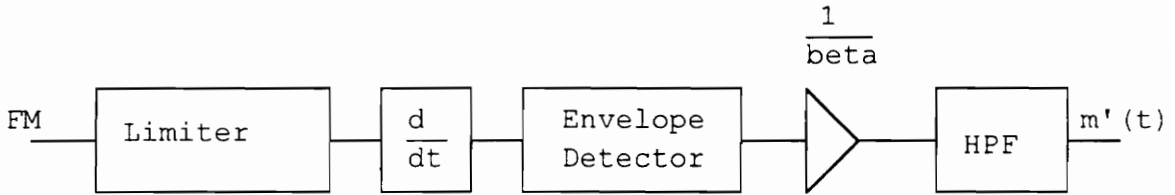


Figure 10. Block diagram for FM-AM frequency demodulator.

The block diagram for this demodulator is given in Figure 10. The initial limiter may be used to eliminate unwanted amplitude modulation due to channel conditions ( $A(t)$  in Equation 8.). The rest of the diagram follows the equations given above plus a gain or attenuation to remove beta and a high-pass filter to remove the DC offset. The results of this demodulator are shown in Figure 11. The high frequency signal in the top plot is the result of the derivative operation. The low frequency component in the top plot is the result of the envelope detector. After the gain (or attenuation) and high-pass filter is applied the original message signal is obtained as displayed in the bottom plot.

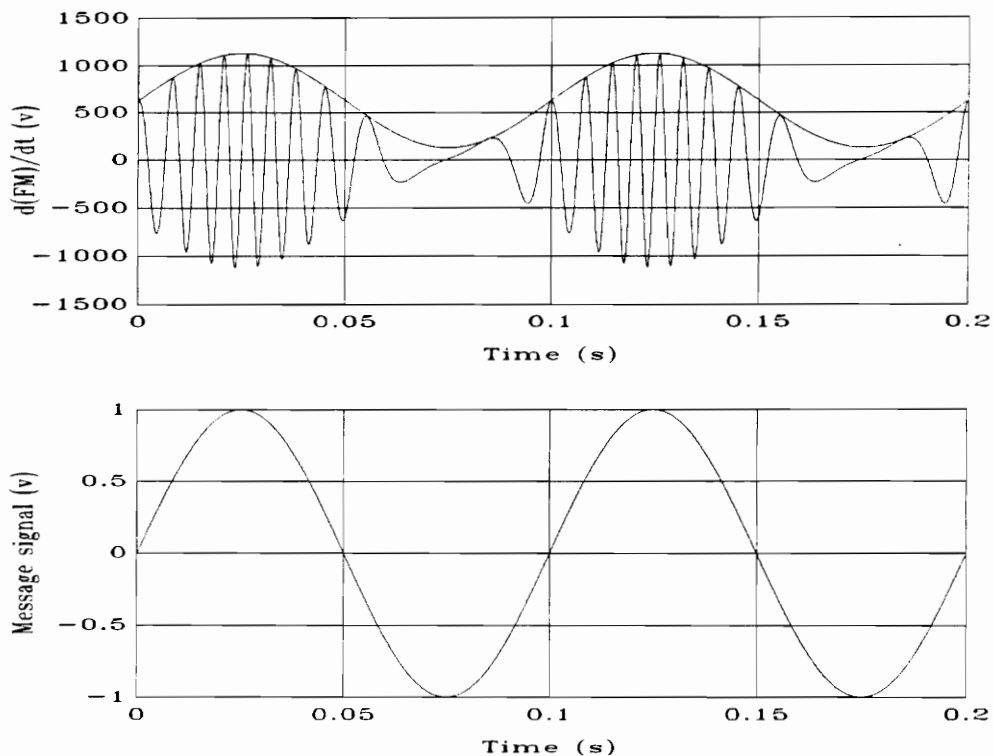


Figure 11. FM-AM conversion for frequency demodulation. Top: Original FM signal and AM signal after FM-AM conversion. Bottom: Original message signal.

## 6.2. Zero-Crossings for Frequency Demodulation

The number of zero-crossings per unit time is linearly proportional to a signal's frequency. An analog technique uses this to demodulate a frequency modulated signal. The block diagram for this demodulation method is given in Figure 12. The limiter converts the incoming FM signal to a binary signal. The monostable multivibrator generates a binary pulse duration  $1/T_c$  on each rising edge of the binary FM signal. The difference between the duty cycles of the output of the monostable multivibrator and its complement is linearly proportional to the

frequency of the incoming FM signal. The duty cycle of each monostable multivibrator output is converted to a voltage level by a low-pass filter. The difference between the resultant duty-cycle voltages is obtained with a difference

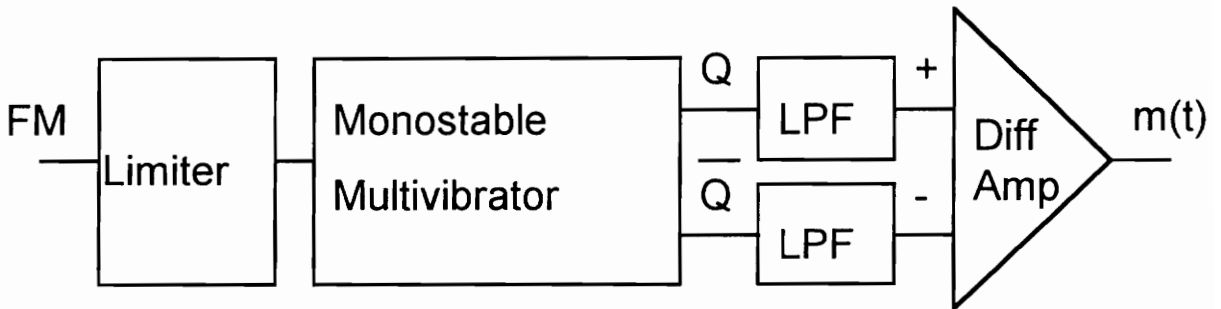


Figure 12. Block diagram for zero-crossing analog frequency demodulator.

amplifier. The gain of the difference amplifier can be set to eliminate the frequency modulation constant resulting in the original message signal.

### 6.3. Phase Locked Loop for Frequency Demodulation

A phase locked loop demodulates a frequency modulated signal by generating a signal that is the same frequency as the incoming signal and looking at the frequency of the generated signal. In Figure 3 the incoming modulated signal,  $g(t)$ , is electronically mixed with the output of a voltage-controlled oscillator (VCO) whose frequency is near the frequency of  $g(t)$ . The mixing produces components at the sum and difference of the two frequencies. The low pass filter removes the sum frequency leaving only the difference frequency which is proportional to the

frequency error between  $g(t)$  and  $vg(t)$ . This then becomes the input to the VCO to change the generated frequency to be closer to the frequency of the incoming signal and to become the output message signal.

A phase locked loop has an acquire region, a hold-in region, and a maximum rate of change of frequency. A phase locked loop will not work without a carrier since the regions mentioned above are some percentage of the carrier frequency. Therefore they are not applicable to the laser vibrometer.

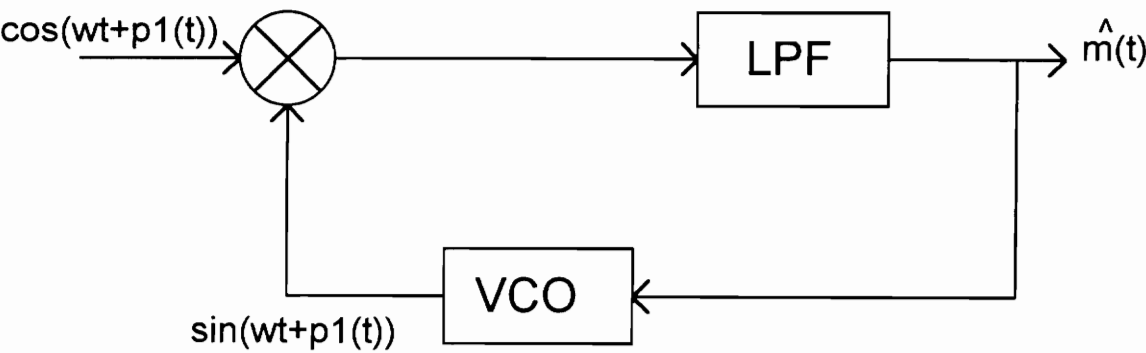


Figure 13: Phase-locked loop for frequency demodulation.

## 7. Digital Frequency Demodulation

In general frequency modulated signals are available as continuous analog signals and traditionally they have been demodulated by continuous analog demodulators. However if the continuous frequency modulated signal is sampled to generate a discrete representation of the signal and then demodulated with digital signal processing the demodulation is a 'digital' frequency demodulation. Each of the analog techniques for frequency demodulation has a digital counterpart and there are some strictly digital techniques that have been introduced. Three digital demodulation methods will be reviewed here.

### 7.1. Why Digital Demodulation?

Before describing each of the digital demodulations in detail it is important to consider why a digital demodulation might be chosen for the laser vibrometer.

One reason for choosing a digital demodulation method is that the laser vibrometer is easily made to generate a set of near-perfect quadrature signals. These signals are ideal for use by each of the digital demodulators about to be reviewed here.

The flexibility of a digital system is also desirable. The characteristics such as the dynamic range and CNR required are functions of the sampling frequency which may be programmable. In addition once the digital signal processing hardware is in place to perform the demodulation, further signal processing such as digital phase-locked loops and digital filters are easily implementable in the same



system. This feature will be exploited in one of the last chapters of this thesis to continuously track the magnitude and phase of the message signal in a sine-dwell vibration test.

An additional feature of at least the RE-TAN digital demodulation method is that phase demodulation or frequency demodulation requires the same basic hardware and therefore can be programmable once the system is developed. It will be seen in this chapter that in at least the RE-TAN case the phase demodulator may be desirable in some if not all cases over the frequency demodulator.

A final extremely important characteristic of the digital frequency demodulation methods is that the dynamic range of these digital demodulators is limited only by the sampling frequency and they have a linear magnitude response and phase response throughout their range.

## **7.2. Comparison Methods**

This section describes the tests that will be applied to each of the digital demodulation methods. The basic test case is a .1m/s velocity and a 10MHz sampling rate. To test these methods they are applied to simulated quadrature Doppler signals for this test case and a frequency modulation constant of  $3.16 \times 10^6$  Hz/m/s. To vary the carrier-to-noise ratios (CNR) for these Doppler signals varying amounts of additive noise are added. The signal-to-noise (SNR) ratio of the generated message signal and the CNR of the Doppler signals are the ratio of the noise power (or variance) to signal power (or variance) for each,

$$\begin{aligned}
CNR[dB] &= 10\log_{10}\left(\frac{\text{carrier power}}{\text{noise power}}\right) = 10\log_{10}\left(\frac{\sigma_c^2}{\sigma_n^2}\right) \\
SNR[dB] &= 10\log_{10}\left(\frac{\text{signal power}}{\text{noise power}}\right) = 10\log_{10}\left(\frac{\sigma_c^2}{\sigma_s^2}\right)
\end{aligned}
\tag{Eq. 13}$$

For each digital demodulation method a signal to noise ratio (SNR) for the output is plotted versus the carrier to noise ratio (CNR) for the input. These plots show two important attributes of the demodulator. The first is the threshold CNR at which the SNR output drops off suddenly. In frequency demodulation theory this is approximately 10dB. This indicates how much noise is allowed on a constant amplitude carrier, or how low the amplitude of the carrier can drop in the presence of constant noise, before the frequency demodulator begins generating poor results. The second demodulator attribute shown in the SNR vs. CNR plot is the magnitude of the SNR output for a given SNR input, which should be as large as possible.

### 7.3. Arctangent-Type Digital Frequency Demodulation

Previously it was seen that phase and frequency modulation are related in that to perform a frequency demodulation a phase modulation could be performed followed by a differentiation. Phase demodulation from a perfect set of quadrature signals is trivial. Referring back to Equation 8, a pair of quadrature phase modulated signals would look like the following,

$$\begin{aligned}
g_I(t) &= A(t) \cos\left(2\pi f_c t + \beta_f \int_{-\infty}^t m(x) dx\right) \\
g_Q(t) &= -A(t) \sin\left(2\pi f_c t + \beta_f \int_{-\infty}^t m(x) dx\right)
\end{aligned}
\tag{Eq. 14}$$

To determine the instantaneous phase of the modulated signals the four-quadrant arctangent function can be used,

$$p(t) = \text{unwrap} \left[ \tan^{-1} \left( \frac{g_Q(t)}{g_I(t)} \right) \right] \quad [\text{Eq. 15}]$$

$$p(t) = \text{unwrap} \left[ \left( 2\pi f_c t + \beta_p \int_{-\infty}^t m(x) dx \right) \% 2\pi \right]$$

where % is used as the symbol for modulo division. The arctangent function must be a four quadrant function in order to generate frequency values over the entire  $2\pi$  radians. The block diagram for the arctangent-type frequency demodulator is given in Figure 14.

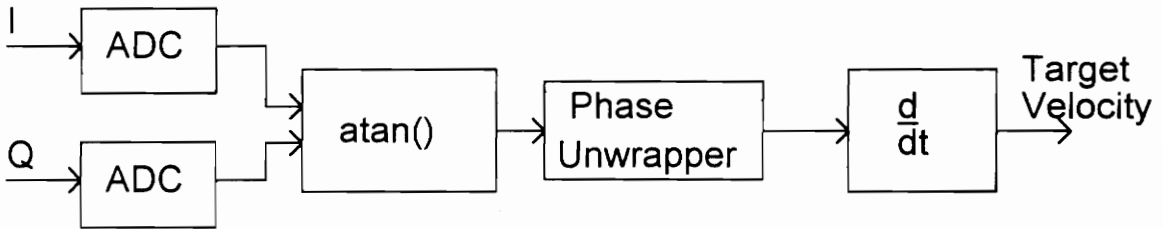


Figure 14: Arctangent-type digital frequency demodulator.

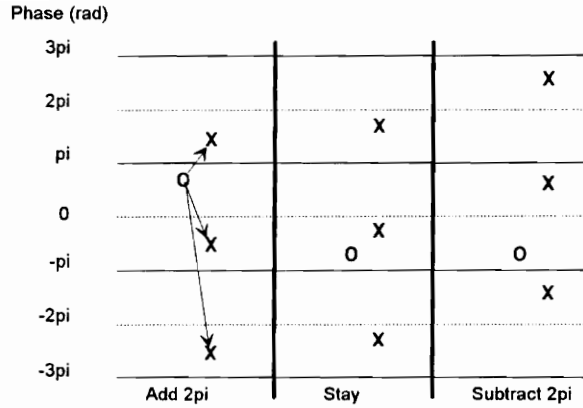


Figure 15: Unwrap point 'x' from 'o' where point 'x' is the current point's phase and point 'o' is the last point's phase. Each 'x' has three possible absolute phases:  $x+2\pi$ ,  $x-2\pi$ ,  $x$ .

The arctangent function returns a modulo- $2\pi$  result that must be 'unwrapped' to obtain the absolute results of the phase demodulator. This unwrapping is not required in the special narrow-band case that the modulated signal never crosses a  $2\pi$  boundary. Some multiple of  $2\pi$  may have to be added after each iteration. In general a nearest neighbor approach is used. Referring to Figure 15, the multiple of  $2\pi$  that minimizes the distance between adjacent phase points is added to  $P(t)$ . This may be implemented in a lookup table or as logic in a programmable logic device (PLD).

It is interesting to describe the unwrapping from a pattern recognition point of view. To perform the phase unwrapping the modulo- $2\pi$  phase for the previous point and the current point are used as features defining a 2-D feature space. Three

classes for each of the possible actions (adding  $2\pi$ , subtracting  $2\pi$ , and staying) are defined as shown in Figure 16.

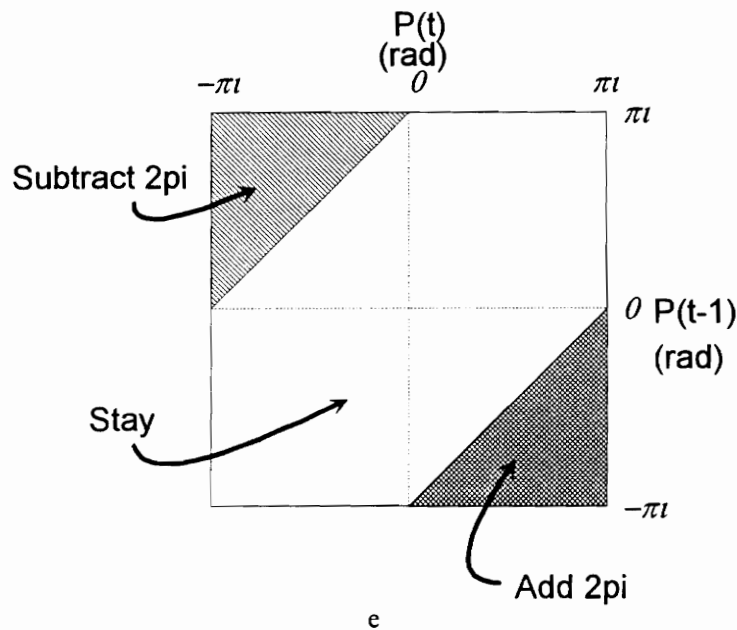


Figure 16. Feature space and classes for phase unwrapping from a pattern recognition point of view. The features are the phase of the current and last point. The classes are 'subtract  $2\pi$ ', 'stay', 'add  $2\pi$ '.

To better understand how the unwrapping works the simulated doppler signals are plotted on the same feature space as used in Figure 16. The four plots of Figure 17 do just that. First the upper left hand plot is considered. Here the sampling frequency is well above the Nyquist frequency and only a small portion of the feature vectors are in the add or subtract  $2\pi$  areas. Referring now to the lower left hand plot, a large amount of noise has been added to the doppler signals.

However due to the extremely high sampling frequency there is a sufficient buffer between classifications so that the probability of a misclassification occurring is small. Looking now at the upper right hand plot, the sampling frequency is lower and there is no noise. Since there is no noise the classes are still obvious however the buffer between classes is considerably smaller. When noise is added, as in the plot in the lower right hand corner, the space between classes disappears and erroneous classifications will occur with high probability.

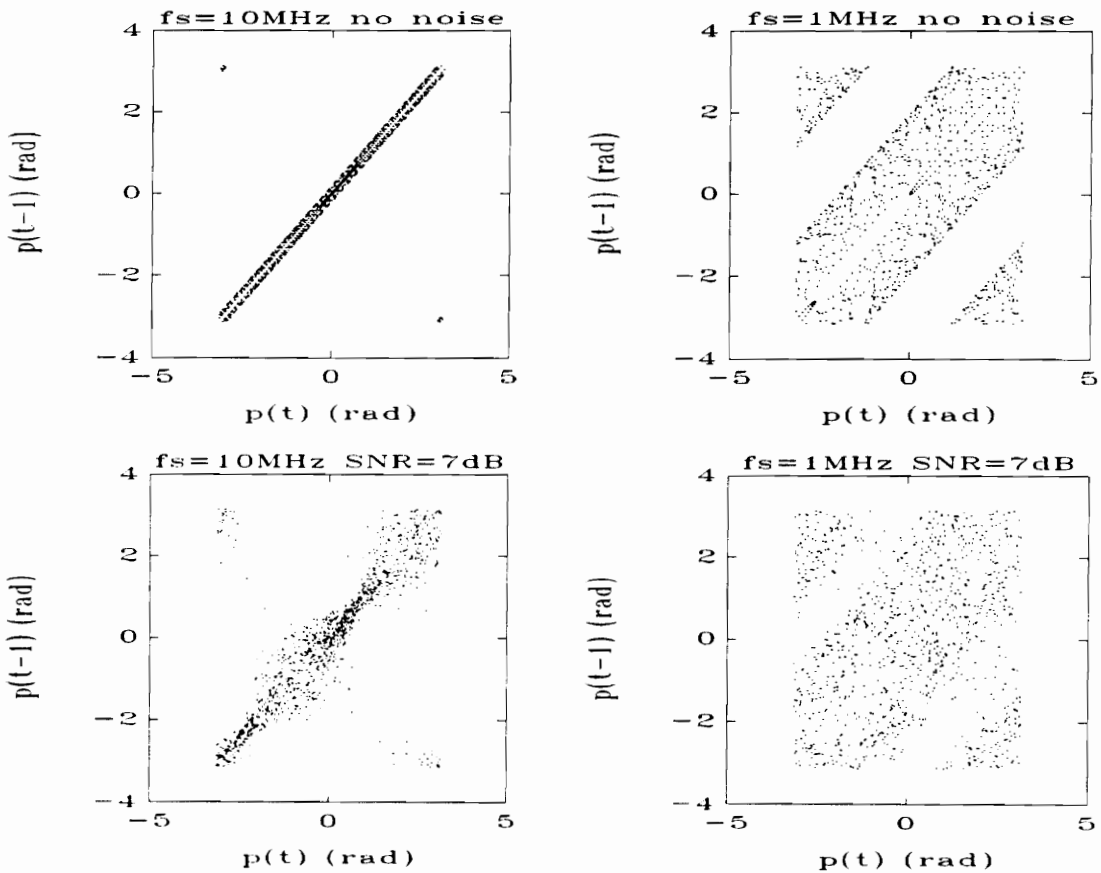


Figure 17. Simulated doppler signal unwrap sample space with different sampling frequencies and with and without additive noise of 7dB SNR.

From the above discussion it is obvious that higher sampling frequencies will lower the acceptable CNR for which phase unwrapping misclassifications will occur with high probability. From this point of view only it would seem that the sampling frequency should be made as high as possible. However higher sampling frequencies lower the SNR of the output.

For an example the simulated Doppler signals will be demodulated. After the arctangent operation the resultant signal looks like the top portion of Figure 18. It is obvious that further processing is required to phase unwrap the result to generate the true phase demodulated signal, shown in the bottom portion of Figure 18. With the carrier frequency term involved one must have a coherent receiver to truly perform a phase demodulation. That is the receiver must be synchronized with the transmitter so that the phase of the carrier frequency term is known at all times and can therefore be eliminated. However it is not necessary for the receiver to be coherent if a frequency demodulation is to be performed. After the derivative the carrier term will be a known constant that can be subtracted out. After performing the derivative to get frequency, subtracting out the carrier frequency term, and dividing by the frequency modulation constant the original message signal is retrieved.

$$m(t) = \frac{\frac{d}{dt}(p(t)) - 2\pi f_c}{\beta_f} \quad [\text{Eq. 16}]$$

For many applications of the laser vibrometer a relative displacement signal is acceptable as an alternative to the velocity signal. Therefore the plot for SNR vs.

CNR is given in Figure 19 for the phase-demodulator and the complete frequency demodulator. It can be seen in the figure that the phase demodulator by itself has a much better SNR vs. CNR function. This of course is due to the differentiator which amplifies high frequency noise.

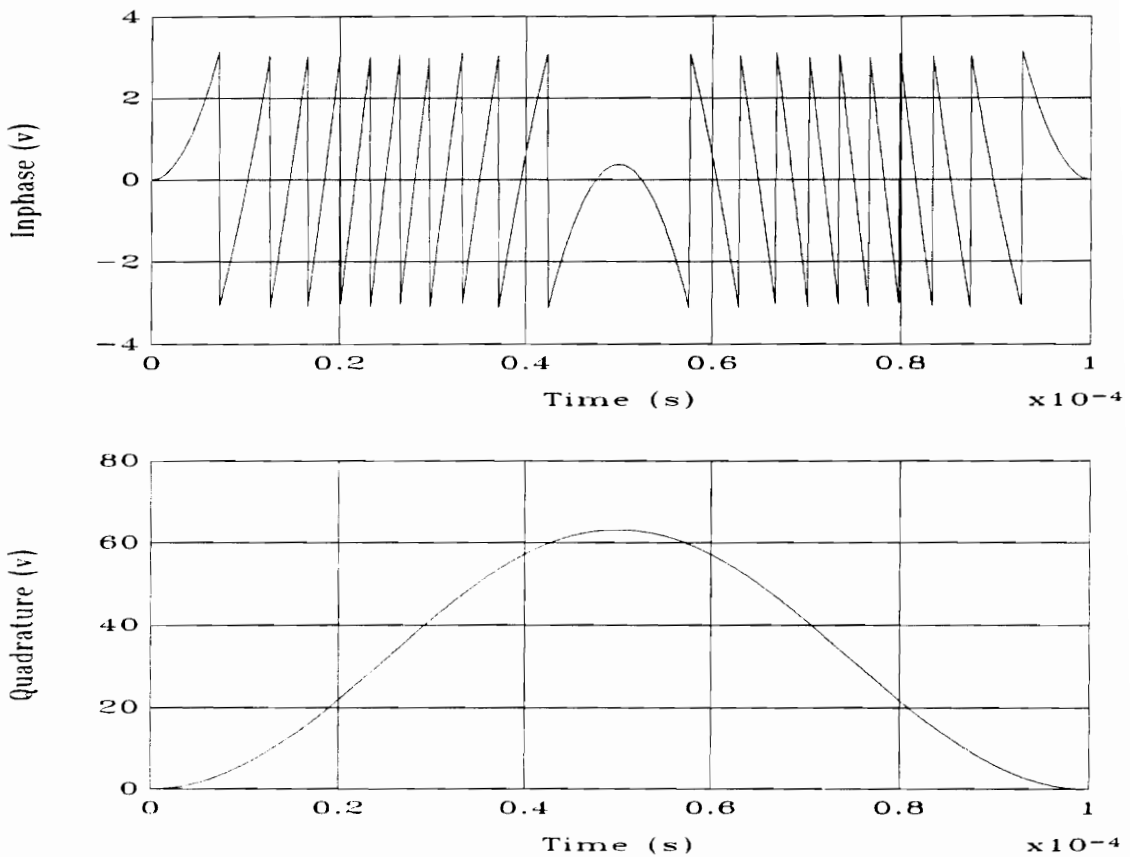


Figure 18. Phase demodulated signal before (top) and after (bottom) phase unwrapping.

With the SNR vs. CNR established the next issue to be addressed is implementability. One of the later chapters addresses this issue in depth so it will



only be touched on here. After the signal is sampled at a high frequency, the arctangent may be performed with a single memory lookup. The phase unwrapper consists of some simple logic and a counter. Each of these elements is easily implemented at high frequencies.

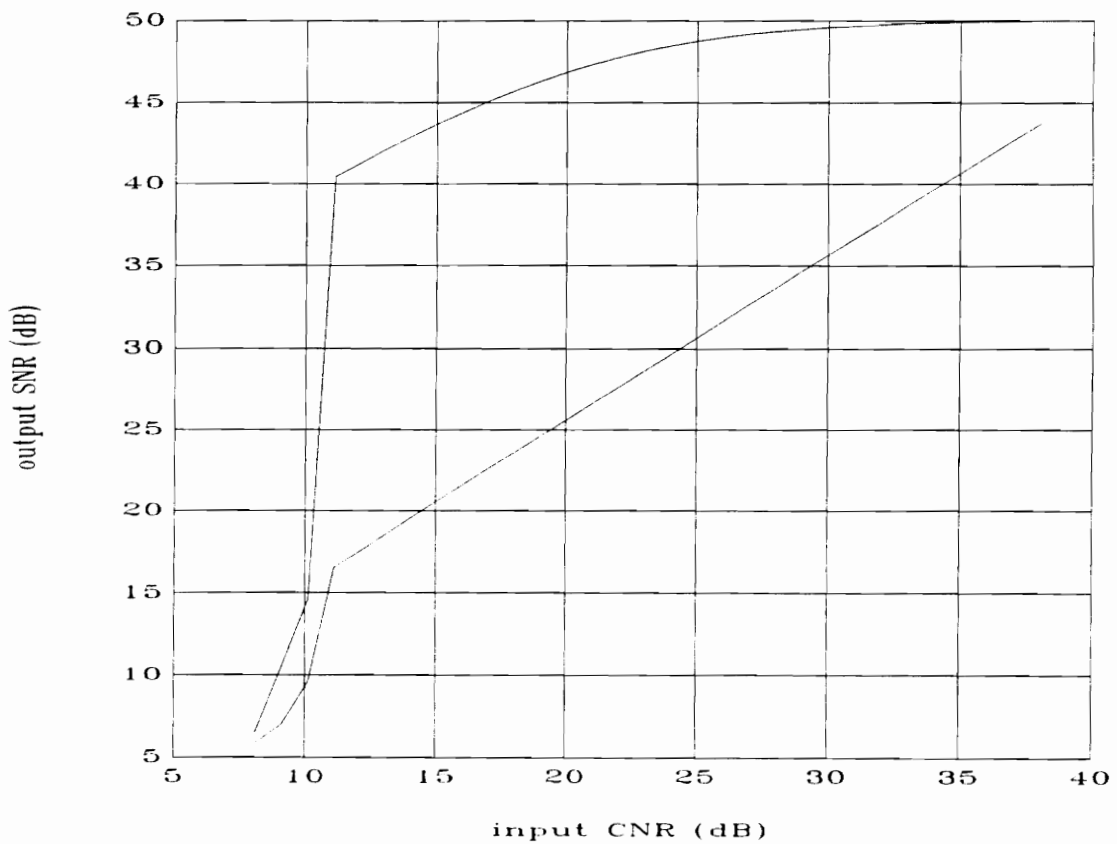


Figure 19. ATAN phase demodulator (top) and frequency demodulator(bottom)

SNR vs. CNR (beta=3.16c6).

#### **7.4. Zero-Crossing Frequency Demodulator**

The analog zero-crossing frequency demodulation method uses the relative duty-cycles of the binary FM signal and its conjugate to determine the frequency of the input signal. A direct digital version of that technique could be used on any frequency modulated signal with a non-zero carrier. However the laser vibrometer generates zero-carrier frequency modulated signal so the analog zero-crossing method is not appropriate. It is possible however to use a slightly different zero-crossing method. To determine the frequency of a sinusoid it is possible to measure the time between its zero crossings and invert to get frequency. If the signal is available in quadrature the frequency may be sampled four times per period otherwise two samples per period can be taken. This method can be implemented with digital techniques on frequency modulated signals at baseband. There are at least two basic approaches to implementing this method. The first uses analog circuitry to recognize zero crossings with digital circuitry performing the calculations to determine frequency. The second method samples the original signal and performs both zero-crossing detection and frequency determination in the digital domain.

The crucial step in each procedure is to determine as accurately as possible where the zero-crossings are. This is simple enough if there is no noise in the system however it becomes more difficult with noise added. To generate a plot of SNR vs. CNR the zero-crossing method implemented by Zeng is used. This method is an all digital implementation that uses interpolation to determine zero-crossing locations and a series of tests to determine sign. From the results in Figure 20 it can be seen that this method has an inferior SNR vs. CNR characteristic compared to

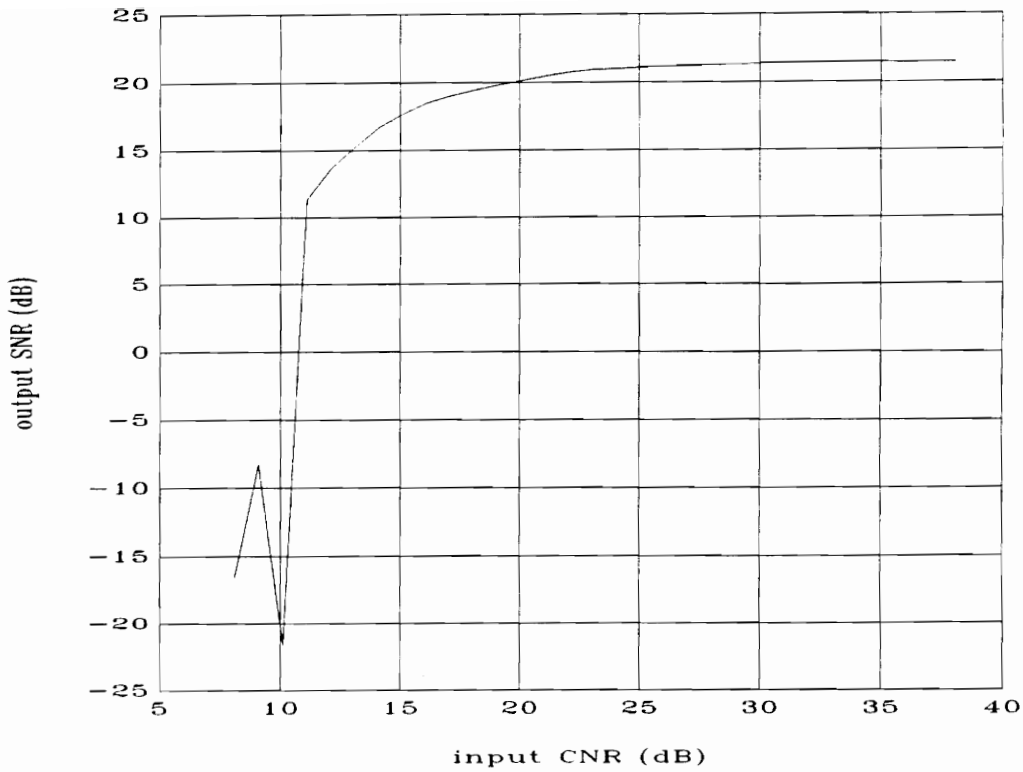


Figure 20. SNR vs. CNR plot for digital zero-crossing frequency demodulation.

the arctangent-type demodulator. The zero-crossing method has a lower SNR for a given CNR than the arctangent-type demodulator.

The actual performance of the zero-crossing method is rather irrelevant in the laser vibrometer case. Implementation of the zero-crossing method in a real time system is not practical, especially when matched against the arctangent-type method.

### 7.5. Balanced Quadricorrelator Frequency Demodulator

The arctangent-method demodulator performed a numerical arctangent to retrieve phase then a numerical differentiator to retrieve frequency. A natural progression is to do the derivative of the arctangent function symbolically,

$$m(t) = \frac{d}{dt} \left[ \tan^{-1} \left( \frac{Q(t)}{I(t)} \right) \right]$$

$$= \frac{I(t) \frac{dQ}{dT} - Q(t) \frac{dI}{dT}}{I^2(t) + Q^2(t)}$$
[Eq. 17]

To implement this requires two differentiators and a division. It should be noted that the linearity of this method depends on the linearity of the differentiators used. The SNR vs. CNR plot for this method is given in Figure 21. This method, like the zero-crossing method, requires a lot of computation to be done at a very high sampling frequency.

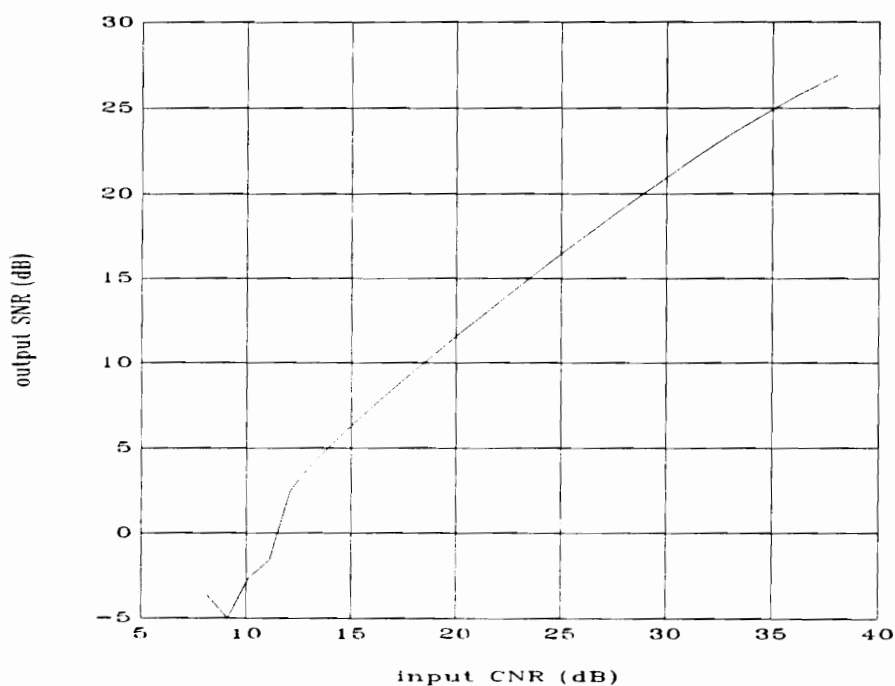


Figure 21. Balanced quadricorrelator SNR vs. CNR (beta=3.16e6).

## 7.6. Demodulator Selection for the Laser Vibrometer

With each of the digital demodulation methods reviewed, one is now selected for the laser vibrometer. To review, the major requirements are real-time or block-mode real-time operation and minimum required carrier-to-noise ratio (CNR). Real time in this case means the demodulator must be able to handle input frequencies of 3.16MHz, the frequency corresponding to a target object velocity of one meter per second. Message signals will have much lower frequencies and are here assumed to be below 30kHz. Finally, it is not necessary to frequency demodulate the signal, a phase demodulation is sufficient.

The issue of required CNR is best looked at in a combined plot of the SNR vs. CNR for each of the digital demodulations presented in the last chapter. From this plot (Figure 22) it can be seen that the arctangent frequency demodulator has the best performance for a given CNR and that each of the demodulation methods falls off at about 11dB CNR. Furthermore the arctangent phase demodulator has a much better performance than all of the frequency demodulators. This is expected since a frequency demodulation contains a differentiation operation that amplifies high frequency noise.

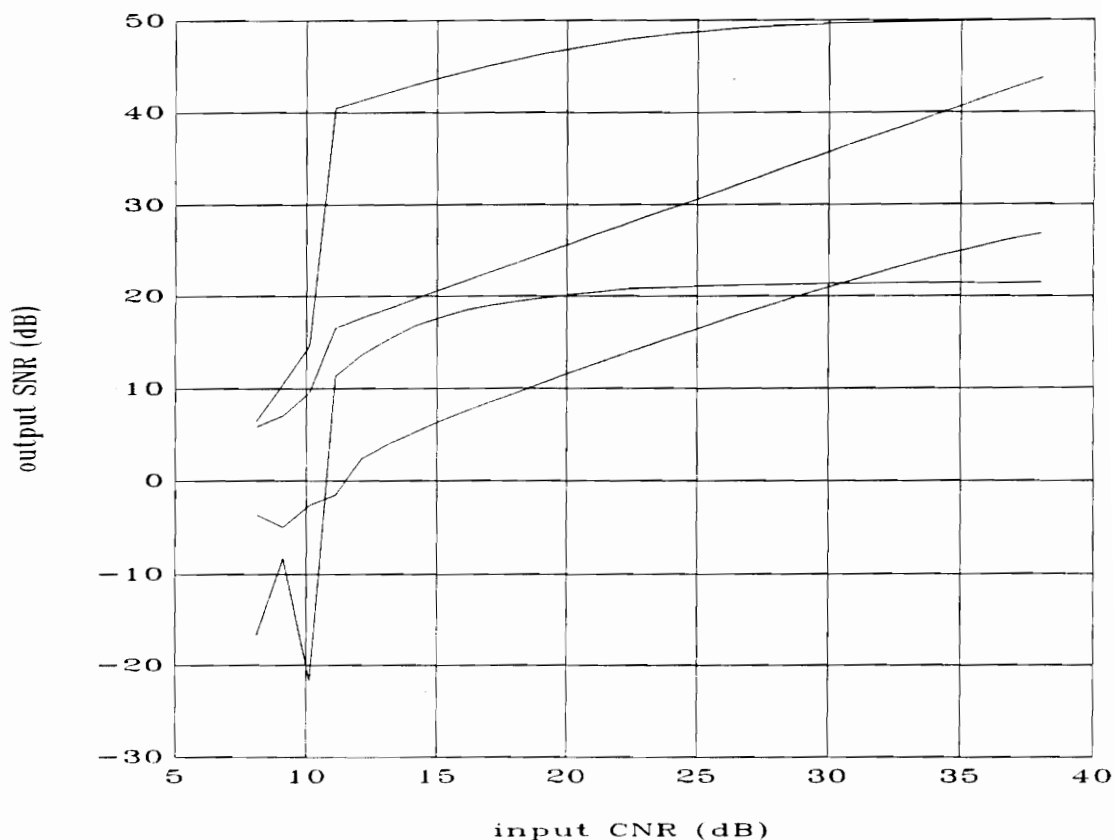


Figure 22. Combined SNR vs. CNR plots for reviewed digital demodulation methods.

On right side from top to bottom: ATAN phase demodulator, ATAN frequency demodulator, balanced quadricorrelator frequency demodulator, zero-crossing frequency demodulator.

The zero-crossing method is not appropriate for real-time implementation since the algorithm for determining zero-crossing locations and calculating the resulting frequency is too complex to operate at 10 MHz with current digital signal processors. In addition the SNR vs. CNR is inferior.

The balanced quadricorrelator has an inferior SNR vs. CNR characteristic to the arctangent-type. It also requires two high speed differentiations and requires seven floating point operations per sample. Also any non-ideal differentiations, such as first difference function approximations which might be implemented at 10 MHz, would create non-linearity in the demodulation.

The arctangent-type demodulator has the highest CNR for a given SNR and can be implemented with minimal high frequency logic. It is important to note that although the arctangent and phase unwrapping must occur at the sampling frequency for the modulated signal, the differentiation may occur at a sampling frequency required for the message signal. In addition, for many applications of the laser vibrometer a phase demodulation is sufficient. This eliminates the noisy differentiation and boosts the SNR vs. CNR characteristic by 20dB over the arctangent frequency demodulation.

For these reasons the selected digital demodulation method is the arctangent-type phase and frequency demodulation. It is these methods that will be focused on during the rest of this thesis.

## 8. Arctangent-type Demodulator Implementation Issues

### 8.1. Sampling Requirements

To satisfy the Nyquist requirement the sampling frequency must be greater than twice the bandwidth of the sampled signal. The doppler signals generated by a quadrature laser vibrometer have a frequency from 0 Hz to the frequency generated by the fastest moving target that will be measured. For the case of a 1m/s target and a 632 nm laser source, the maximum doppler signal frequency is 3.16 MHz. For these frequencies a sampling frequency on the order of 10 MHz is required.

Quantization will add noise to the modulated signal and thus reduce the CNR. From Oppenheim [9] the added noise power (variance) for given signal quantized to B bits is

$$\sigma^2 = \frac{2^{-2B} A^2}{12}$$

$\sigma^2$  = Added noise power. [Eq. 18]  
 $A$  = Full amplitude of quantizer .  
 $B$  = Number of quantizer bits.

for the exact CNR generated by a certain quantization the reader is referred to a standard text such as Oppenheim [9] which gives a SNR (CNR for this case) calculation of,



$$SNR \approx (6B - 1.25) \text{decibels}$$

$$B = \# \text{ bits}$$

[Eq. 19]

This equation requires the sampled signal to fully span the quantization region of the analog to digital converter (ADC). High sample frequency (>10 MHz) 8-bit ADC are readily available and inexpensive.

## 8.2. Phase Demodulator

The phase demodulator, the arctangent function, must execute at the sampling frequency. To do this a look-up table implemented in a ROM may be used and will easily operate at 10MHz. For 8-bit quantization a 64k lookup table is required.

## 8.3. Phase Unwrapping (overflow)

The phase unwrapper is the key element of the arctangent-demodulator and the component that requires some system control during operation. The basic logic to determine when a phase unwrap is required is well defined and easily implemented in the same type of ROM used for the phase demodulator. This logic, being a simple set of Boolean equations, can however be implemented in a single programmable logic device (PLD).

The logic of the unwrapper controls a counter that counts the number of phase unwraps that have occurred. This counter has a finite word length and is therefore guaranteed to overflow at some point. For this reason some higher level processing and control must keep track of the state of the counter and reset it periodically. Depending on the sophistication of the controller this reset will either

appear as a spike on the velocity or relative position output, or it will be passed by seamlessly on the velocity output.

If a velocity output is selected and a processor is used to generate the velocity from the relative position signals generated by the arctangent phase demodulator, then the processor may also work in a pseudo-block mode when the counter nears overrun. Before the counter overruns the processor resets the phase demodulator and records which samples are pre- and post-reset. If a finite impulse response (FIR) differentiator is used to generate the velocity signal, then the processor can keep the inputs to the differentiator continuous by keeping the entire block of inputs to the FIR filter at the pre- or post-reset values. To do this it may have to add the correction to only a portion of the filter inputs at a time. This processing would have to occur at over twice the message signal bandwidth, which is within the capability of digital signal processors in 1994.

#### **8.4. Differentiation**

If a velocity output is desired then a differentiation operation must be performed after the phase demodulator.

It should be noted that Hagiwara chose to put the differentiator before the phase unwrapper in his range extended arctangent frequency demodulator. In that case the phase demodulator is not separable from the frequency demodulator. Hagiwara may have intended for the differentiator to remove any DC components which would cause the counter to overflow. However in a continuous system with a finite word length the counter will overflow eventually even with the differentiator before the phase unwrapper. Furthermore, as Boutin pointed out, the differentiator

will add noise to the signal going to the phase unwrapper and therefore raise the minimum carrier-to-noise ratio threshold for which the demodulator will work.

If the differentiator for the laser vibrometer is applied at the original sampling frequency of 10MHz then the message signal would certainly be in the region of the first difference function that closely approximates the true first derivative. With a special multiplier-accumulator chip, this may be the way to go. However a digital signal processor working closer to the message signal sampling frequency would be able to closely approximate the first derivative with a higher order difference function and would also allow other types of digital signal processing to occur. For instance the relative position signal may be generated, or the velocity signal, etc. The next section will make additional use of this processor to further extend the capabilities of this demodulator for the case of a single sinusoidal message signal.

## 9. Post-Demodulation Velocity Tracking

This chapter derives a digital demodulator that is specific to a sine-dwell vibration test. In these tests the target has a velocity that is sinusoidal at a known frequency and the response of the structure at that frequency is the only information to be extracted. In particular the magnitude of the response and phase difference between the excitation and response is required. For this test it is important only to extract the magnitude and phase of the velocity component at that single frequency.

### 9.1. Proposed Configuration

For the sine dwell case the proposed configuration consists of a quadrature detector and a local oscillator that will track the velocity signal. The local oscillator or its magnitude and phase parameters will be the output of the frequency demodulator for the sine-dwell frequency demodulator. There will be an additional signal, referred to hereafter as the 'quality' signal, internally generated and used by this demodulator that is an indicator of the quality of the frequency modulated signals used to generate the velocity signal. If the quality signal is above an acceptable threshold then the point estimates for magnitude and phase given by the quadrature detector will be used for the magnitude and phase of the local oscillator. However if the input signal quality is poor, then the local oscillator parameters will not change and the resultant velocity signal will not suffer the effects of a laser dropout since the local oscillator will continue generating a velocity signal with the last 'good' parameters. Of course if the actual velocity signal changes during this period, it will not be tracked correctly. However in a sine dwell test the velocity

signal is not expected to change during data acquisition. The diagram for this configuration is given in Figure 23.

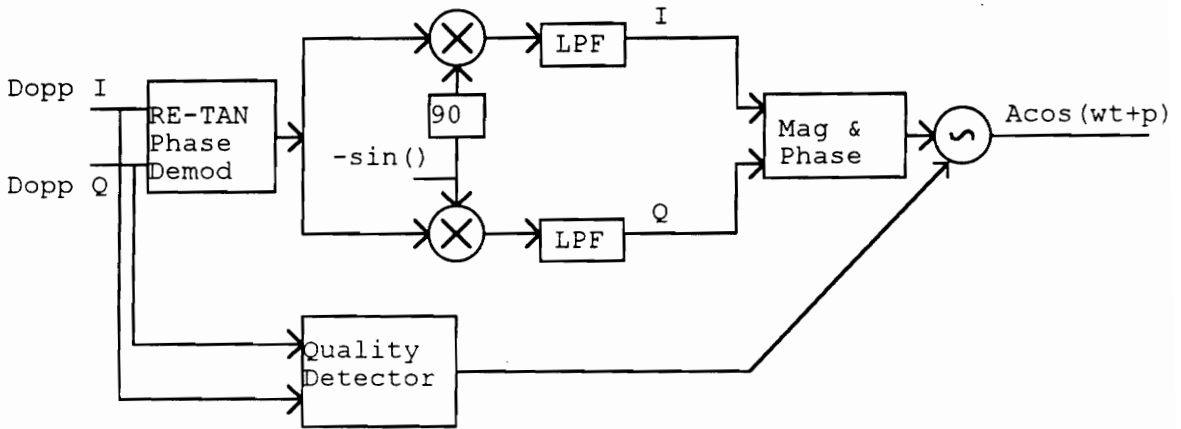


Figure 23: ATAN demodulator for a sine-dwell test.

This local oscillator approach is quite similar to a phase locked loop but there are some significant differences. First it is obvious that the proposed local oscillator approach is not a loop at all since there is no feedback in the system. A phase locked loop attempts to synchronize a local oscillator with an input signal through feedback. The local oscillator applied here is slaved, in an open loop configuration, to the instantaneous magnitude and phase values generated by the quadrature detector if the input signal quality is sufficient. Referring back to the SNR vs. CNR plot for the RE-TAN phase demodulator, it can be seen that if the input CNR is acceptable then the output will be a high quality signal. Also, if only a single frequency exists in the velocity signal then the quadrature detector will

provide high quality magnitude and phase estimations. For these reasons the open-loop configuration of the proposed method is justified.

Note that in the proposed configuration the RE-TAN phase demodulator is used, not the frequency demodulator. This is because for the sine-dwell test it is irrelevant whether relative position or velocity is generated. After the magnitude and phase of the relative position are generated they can be differentiated to obtain velocity and differentiated again to obtain acceleration. Since it is trivial to perform the differentiation after the point estimates for magnitude and phase are made, it makes sense to take advantage of the higher SNR vs. CNR characteristic for the phase demodulator compared to the frequency demodulator.

In order for the proposed configuration to work two key components must be designed. The first is the low-pass filters used in the quadrature detectors and the second is the frequency modulated signal 'quality' detector. Before these components are designed the signal's generated by a typical sine-dwell test will be examined.

During a typical sine-dwell test the target object is excited at some known frequency and the laser vibrometer is used to measure that velocity. This basic model is straightforward however there are additional complications in the real system.

It must be remembered that the laser vibrometer is sensitive to displacement changes on the order of 1nm. In any test setup there are external influences that cause the distance between the laser vibrometer and the target to change. These include but are not limited to floor vibrations, air flow in the test environment, and

conceivably even movement in the scanning mirrors of the vibrometer itself. On top of this there are normal sources of additive noise in the system and of course the large multiplicative noise due to laser speckle. Each of these noise sources cause relative position signals to exist at frequencies other than the desired excitation frequency. To design the sine-dwell modulator these noise sources must be recognized.

Before continuing it must be stressed that each test setup for the laser vibrometer is extremely different and therefore there can be no quantitative description of noise sources in the test. Even within the same test setup, if the laser is pointed to a different location on the target the noise sources in the system could be completely changed. Therefore the components for the sine-dwell demodulator are designed with only rough estimates of noise sources in mind.

First, the additive noise at the output of the phase demodulator is assumed to be a constant additive white Gaussian noise (AWGN). Since the phase demodulator has a very high SNR vs. CNR characteristic the additive noise is barely visible in Figures 24 and 25 which are plots of actual Doppler signals taken with a He-Ne laser vibrometer.

Second it is assumed that external influences such as air flow will introduce very low frequencies to the system. A low frequency movement can be seen in Figure 24 which is a plot of the demodulated relative position.

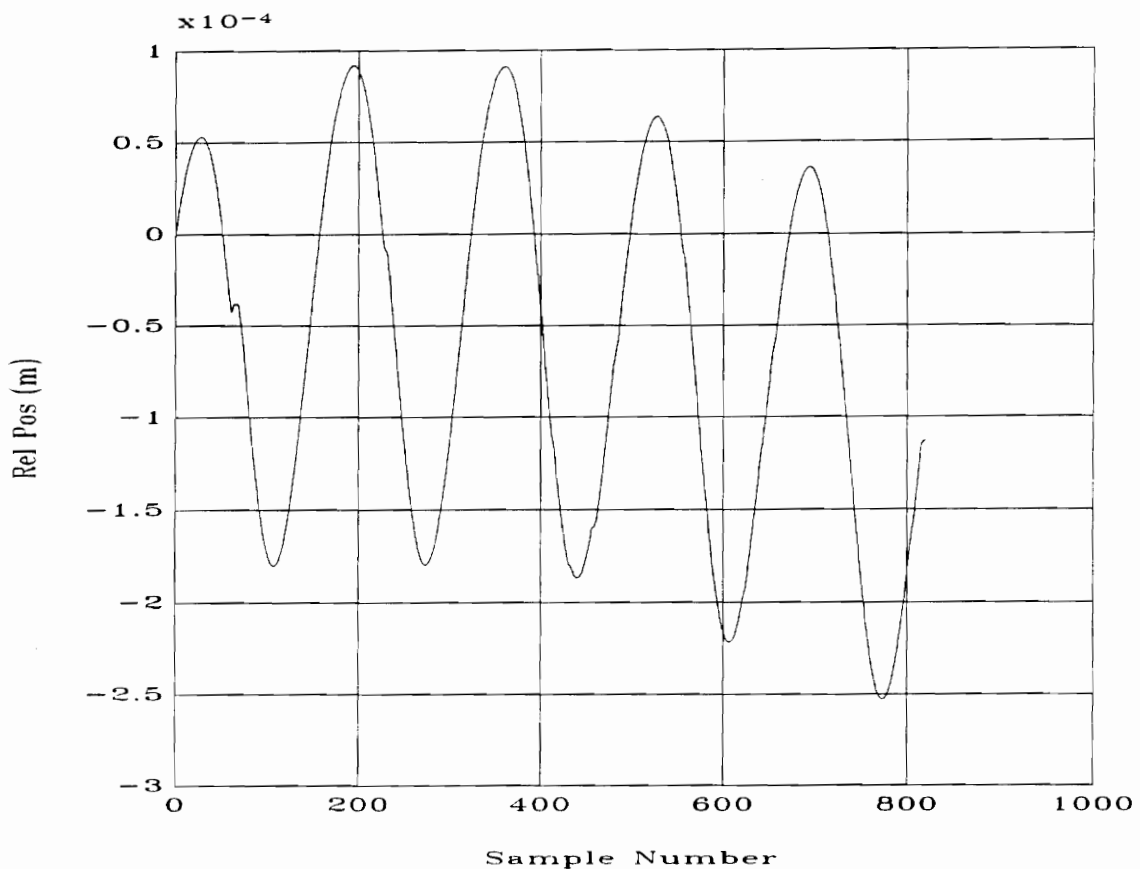


Figure 24. Relative position signal showing low-frequency movement in addition to excitation movement.

Finally it is recognized that laser dropout will cause an unacceptably low CNR on the Doppler signals at some point during the demodulation. This will in turn cause the phase demodulator output to be undefined. However in trials with real data the result is a flat spot. This flat spot can be viewed as adding two 'step' functions to the relative position signal at the beginning and end of the dropout. Basically, a DC offset is added to the demodulated signal during the dropout. The effect of the dropout can be seen around sample 80 in Figure 24 and a larger dropout can be seen in Figure 25 at about sample 650. In Figure 25, which shows the doppler signals as well as the phase demodulated relative position, it can be seen



that the dropouts do indeed occur when the Doppler signal amplitudes are very small.

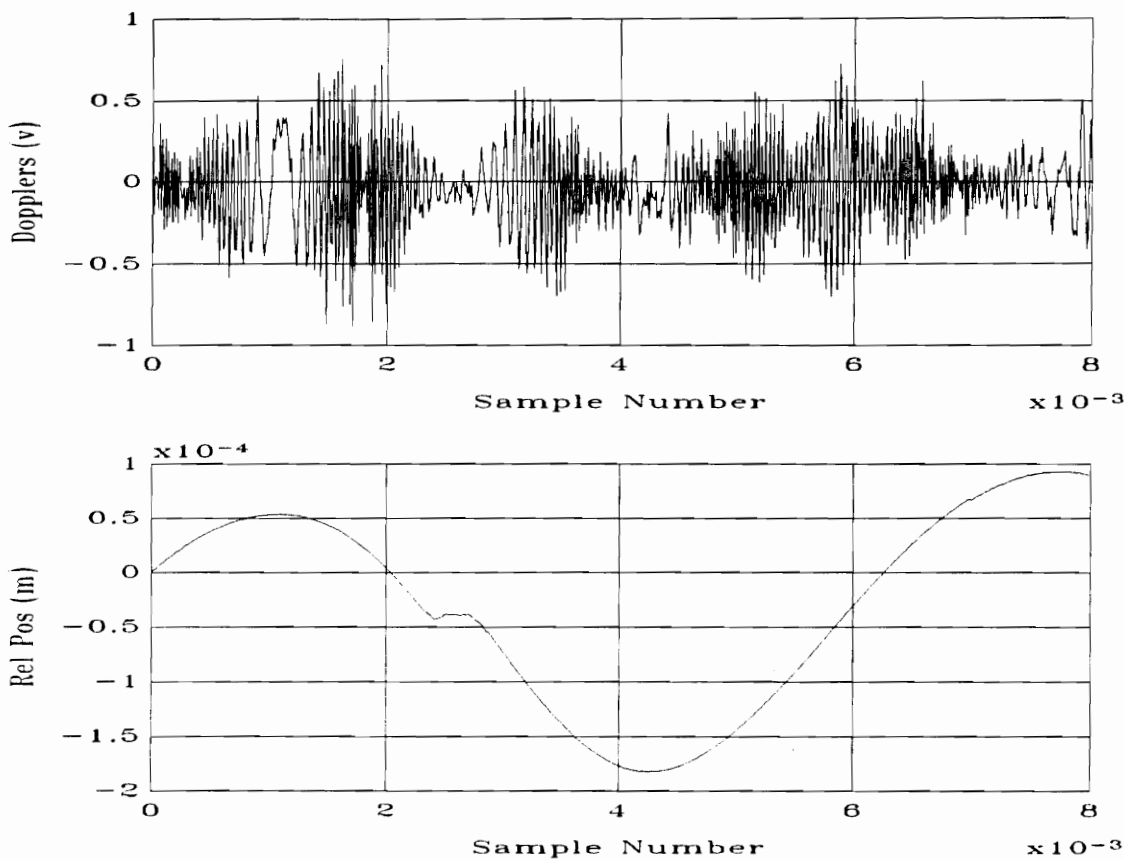


Figure 25. Doppler signals with ATAN phase demodulated relative position signal.

**9.2. Quadrature Detector LPF Design**

With ideal components the quadrature detector used in the proposed sine-wave demodulator will eliminate all sources of noise except those at the excitation

frequency. However since the components are not ideal other noise sources will affect the quality of the magnitude and phase estimates made by the quadrature detector. The low-pass filters will determine the ability of the system and they have two major characteristics that must be taken into account. The first bandwidth which should be made as small as possible to minimize the amount of noise passing through the quadrature detector. The second is the settling time which will dictate how quickly an accurate estimate for magnitude and phase can be obtained. It will also be seen later that a minimum settling time will ease the laser dropout problem after the quality signal is applied. This section designs the low pass filters to be used in the quadrature detector. Throughout this section laser dropout is not taken into account. The next section is dedicated to that problem.

The quadrature detector works by first multiplying the input signal by  $\cos()$  and  $-\sin()$ . This process shifts the input signal so that the excitation frequency is at baseband and it generates a quadrature representation of the signals. However noise sources are also shifted. From the previous section it can be assumed that the input relative position signal consists of a response component at the excitation frequency but also some low-frequency components and white noise,

$$p(t) \approx A_1 \cos(\omega_e t + \theta_e) + A_2 + n(t)$$

where,

$A_1$  = Amplitude of response

$\theta_1$  = Phase of response

$\omega_e$  = Excitation frequency

$A_2$  = Amplitude of near -DC components

$n(t)$  = Additive noise

[Eq. 20]

Looking only at the in-phase component of multiplication by  $\cos()$  the result is,

$$\begin{aligned} 2 \cos(\omega_e t) p(t) &= 2 \cos(\omega_e t) (A_1 \cos(\omega_e t + \theta_e) + A_2 + n(t)) \\ &= A_1 \cos(\theta_e) + A_1 \cos(2\omega_e t + \theta_e) + 2 A_2 \cos(\omega_e t) + n(t) \end{aligned}$$

[Eq. 21]

Note from the last equation that after the multiplication that the desired component is exactly at DC and the others are at approximately the excitation frequency (only approximately since the low-frequency components are only approximately at DC) and exactly twice the excitation frequency. The designed low-pass filter should eliminate the components at the excitation and twice the excitation frequency and minimize the additive noise problem.

The main concern in designing the low-pass filters for the quadrature detector is to remove all components at the excitation and twice the excitation frequency. A simple and effective method of doing this is to place filter zeros at

those locations. Since the filter is digital and therefore reprogrammable within the system for each test, this is possible. This requires a total of four zeros for a fourth order real (as opposed to imaginary) digital filter which is thus far a finite impulse response (FIR) filter.

In order to minimize the additive noise that is passed through the low-pass filters their bandwidth should be minimized. A smaller bandwidth comes at a price of greater order and therefore group delay which in turn means longer acquisition

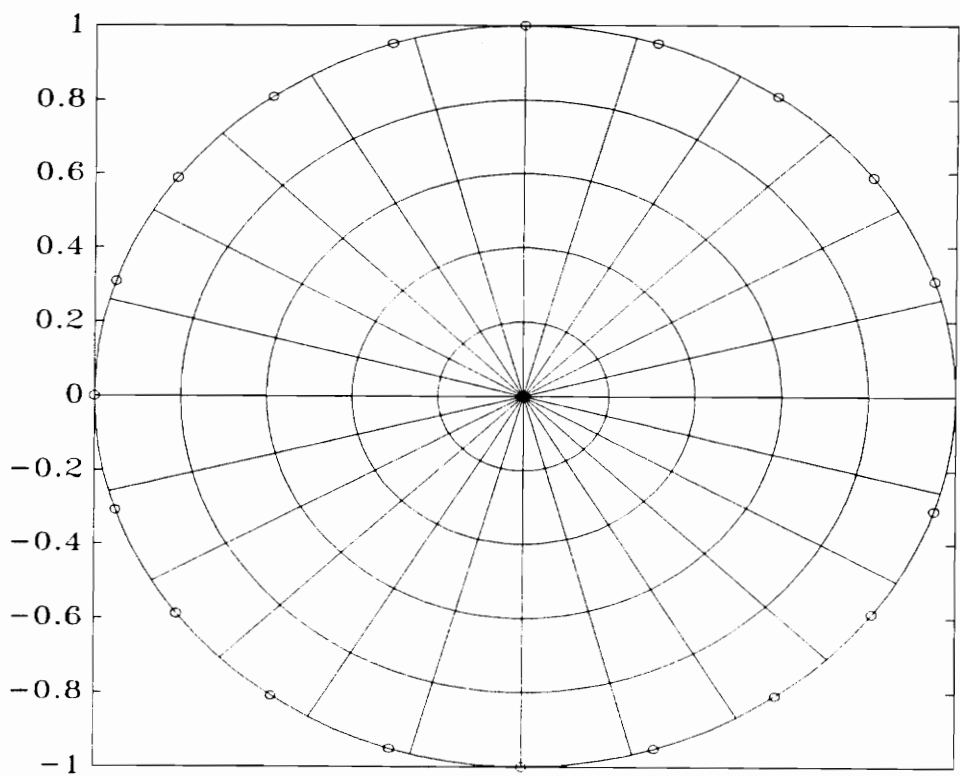


Figure 26. Zero plot for the designed quadrature detector low-pass filters.  $f_e=f_s/20$ .

times. An acceptable solution to the filter design requirement is to place zeros at multiples of the excitation frequency over the entire range from zero to the half-sampling frequency including the half-sampling frequency. A zero plot for this filter on the unit circle in the Z-domain is shown in Figure 26.

A plot for the magnitude characteristic for this filter when the excitation frequency is 1/20 of the sampling frequency is shown in Figure 27.

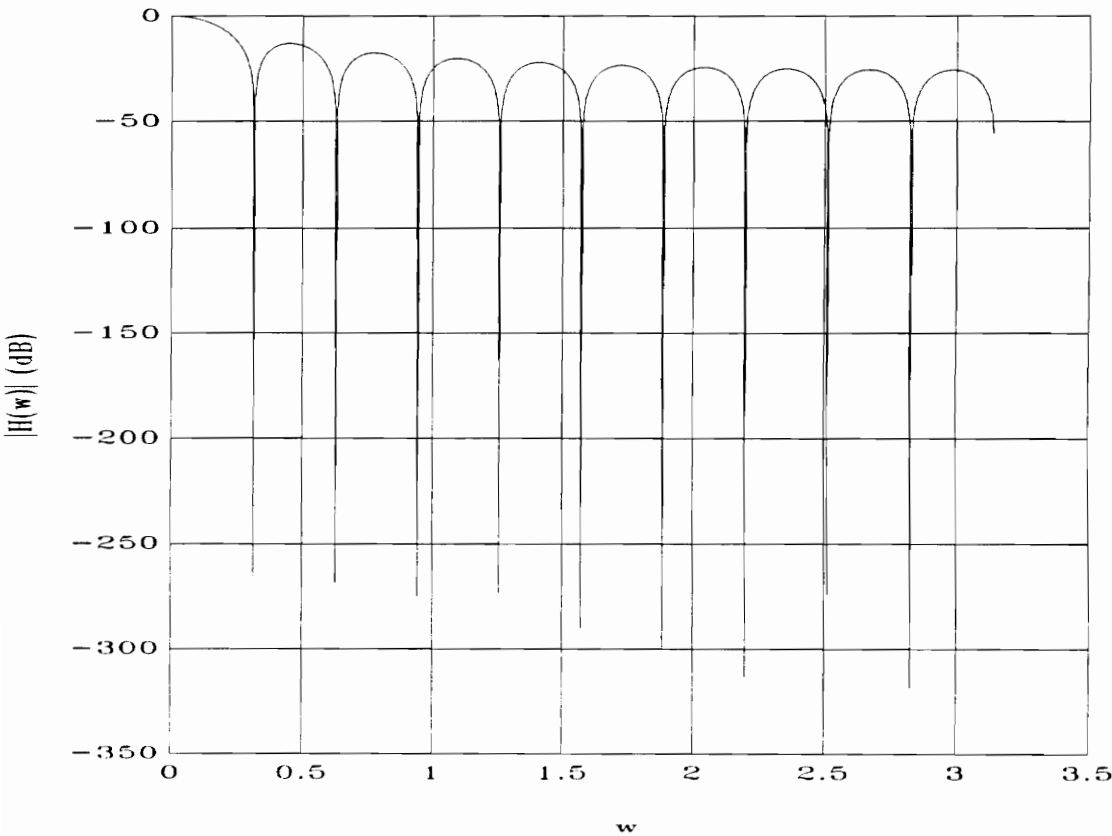


Figure 27. Magnitude characteristic of designed quadrature detector LPF.  $f_e=f_s/20$ .

### 9.3. CNR Dropout Detection

For the sine-dwell demodulator proposed earlier in this chapter to work properly, the quality signal must accurately predict when acceptable Doppler signals are available to the phase demodulator. From the plots of output SNR vs input CNR for the arctangent-type phase demodulator it can be seen that an input CNR greater than approximately 15dB is required for an acceptable SNR on the output. Due to the laser speckle dropout problem the Doppler signal power will drop out for a short time periodically. Assuming the additive noise is constant, during the dropout the ratio between Doppler signal power and noise power drops, possibly to levels under 15dB where the phase demodulator is no longer effective. Therefore the Doppler signal power without noise can be used as an indicator of CNR. Of course the only Doppler signals available have noise with them so only an approximation to the Doppler signal can be obtained. Various approaches to generating an easily computed effective signal that indicates Doppler signal power and CNR are possible. Some are reviewed in the next sections.

### 9.4. Magnitude of Doppler Quality Signal

Neglecting noise on the Doppler signals, their amplitude may be determined with the basic identity,

$$A_d = \sqrt{DoppI^2 + DoppQ^2} \quad [\text{Eq. 22}]$$

The dropout shown in Figure 25 is plotted again in Figure 28 with this Doppler signal amplitude indicator. From the figure it can be seen that the magnitude of the

doppler signals may be used as an indicator of signal quality. Dropouts occur only at points where the magnitude of the doppler signals fall below 0.2. At this threshold there will be false alarms but this should be acceptable. Indeed only a single high-quality estimate of magnitude and phase is actually required. Although the magnitude of the Doppler signals is an acceptable indicator of signal quality its computation may be complex and therefore the search for an alternative indicator should continue.

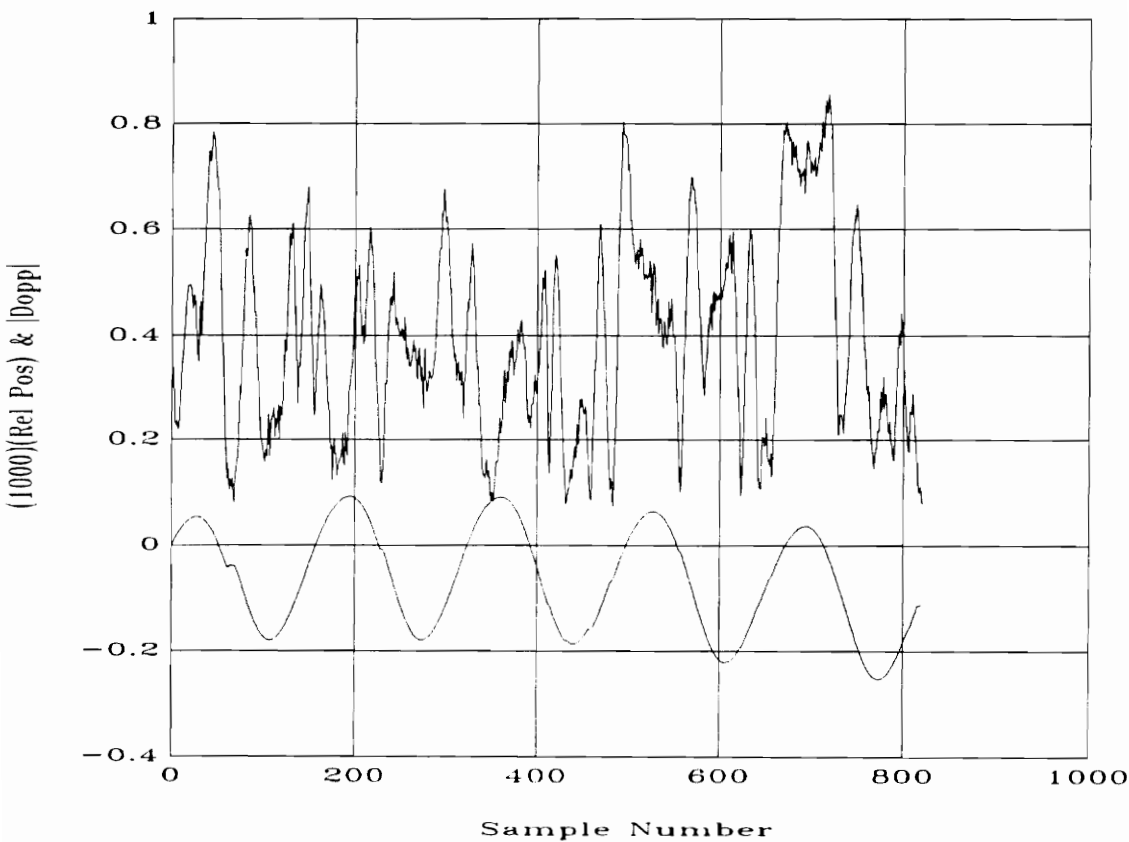


Figure 28. Magnitude-of-Doppler quality signal with relative position signal.

### 9.5. Sum of Doppler Absolute Values Quality Signal

An alternative quality indicator to the magnitude of the Doppler signals is the sum of the absolute values of each Doppler signal,

$$q = |DoppI| + |DoppQ| \quad [\text{Eq. 23}]$$

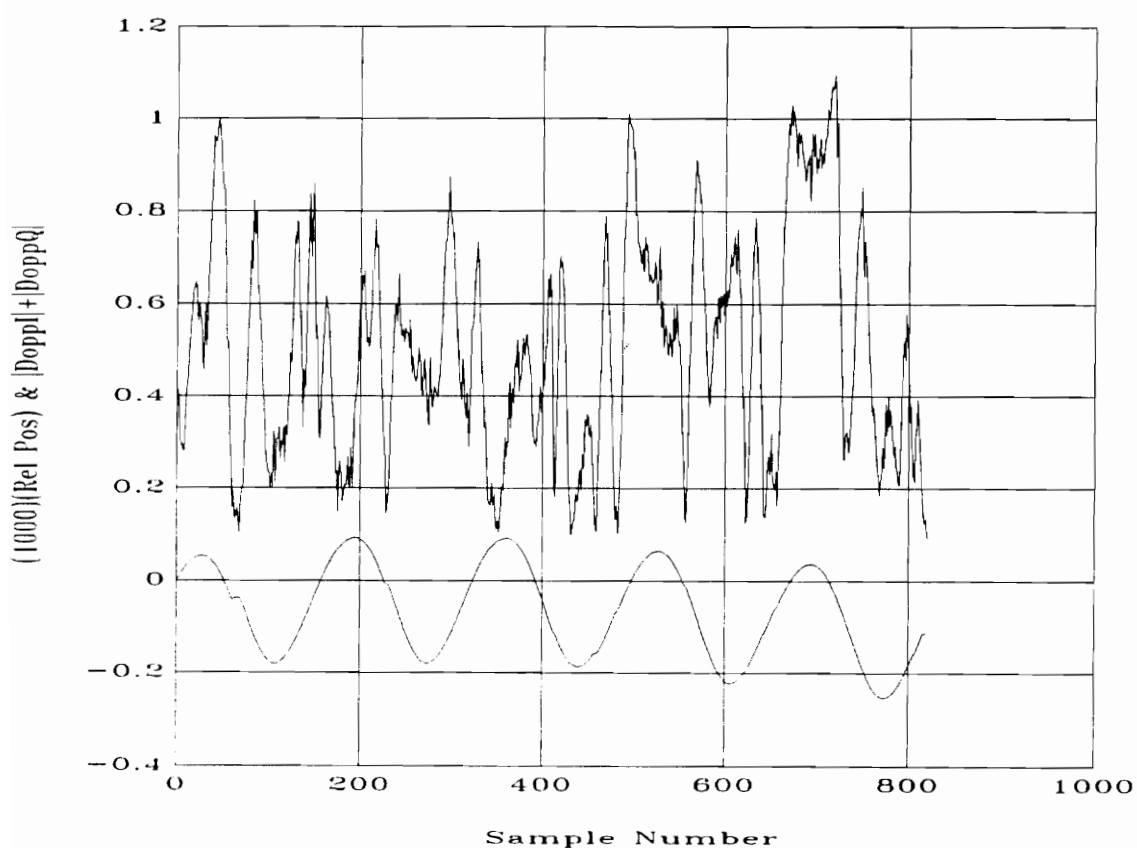


Figure 29. Sum-of-Doppler-absolute-values quality signal with relative position signal.



The plot for this indicator is given in Figure 29. Note that the sum-of-absolute-value signal is quite similar to the Doppler magnitude signal. Again, for a given threshold, there will be false alarms where the magnitude and phase of the quadrature detector is not used although it could be. The benefit of this characteristic is that it may be implemented with two full-wave rectifiers and a summer.

### **9.6. Application of the Sine-Dwell demodulator**

In this section the sine-dwell demodulator is simulated, first without and then with the quality signal.

After application of the RE-TAN phase demodulator, quadrature detector, and local oscillator the output of the sine-dwell demodulator is shown in Figure 30. Also shown is the raw relative position before the quadrature detector and local oscillator are applied. The figure shows that while there is decent signal quality the sine dwell demodulator will work effectively. However during a laser dropout the magnitude and phase estimates are erroneous. It is for this reason that the quality signal should be applied to detect when the Doppler signals have a sufficient CNR to generate correct magnitude and phase estimates.

With the magnitude-of-Doppler and sum-of-Doppler-absolute-values quality signals available, the issue of applying them to the proposed sine-dwell demodulator rises. During this derivation, only the sum-of-Doppler-absolute-values quality signal will be used and it will be referred to only as the 'quality' signal.

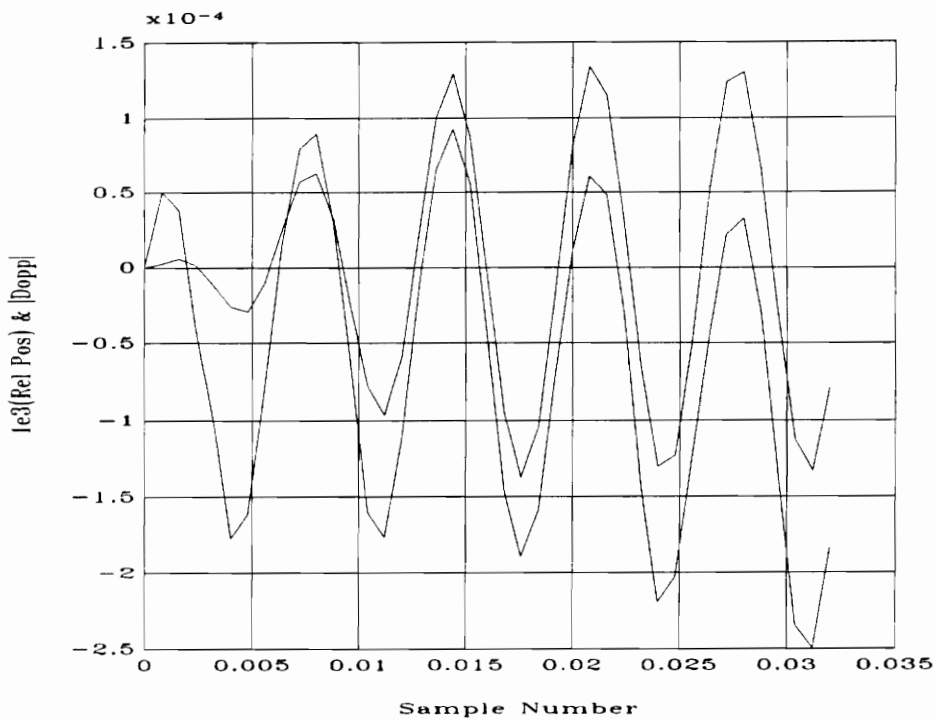


Figure 30. Relative position signal generated with phase demodulator (lower on right) and full sine-dwell demodulator (higher on right).

To apply the quality signal there must be a decision of whether or not the quality signal suggests that the input Doppler signal CNR is sufficient for an effective phase demodulation. To do this the quality signal is thresholded. If the quality signal is above a certain level, then the Doppler signal CNR is considered to be acceptable and the point estimates for magnitude and phase from the quadrature detector are applied to the local oscillator. If however the quality signal is below the given threshold then the point estimates from the quadrature detector are not used

and the estimates from the last valid point are kept, with of course the time-varying nature of the phase at the excitation frequency taken into account.

As stated earlier in the original description of the sine-dwell demodulator and shown in Figure 23, the quality signal dictates whether the point estimates of magnitude and phase generated by the quadrature detector will be used for the local oscillator or whether the parameters to the local oscillator will remain unchanged.

To illustrate this approach a simulation was run that generated Doppler signals for a known message signal. The Doppler signals were given a sinusoidal amplitude modulation then noise was added to the signals. The plot for the magnitude estimate from the local oscillator with and without the quality signal applied is shown in Figure 31. In this figure the estimated magnitude should be a constant 0.1 once the settling time of the low-pass filter is achieved. However simulated dropouts cause the quadrature detector to produce incorrect results which appear as dips in the estimated fit. With the quality signal applied the estimated magnitude for a given point is used only if the quality signal is above a certain threshold. For this reason the estimated magnitude remains constant for a period of time while the quadrature detector produces erroneous results. However once the quality signal is above the threshold again the quadrature detector still produces erroneous results since its low-pass filter is still using some of the poor points in generating the current estimate. To get past this problem the quality signal must remain at an acceptable level for the  $N$  points previous to the current point where  $N/f_s$  is the settling time for the low-pass filter. With this condition the estimated magnitude remains at 0.1 as it should. This effect is another reason why the low-pass filter should have a minimum settling time.

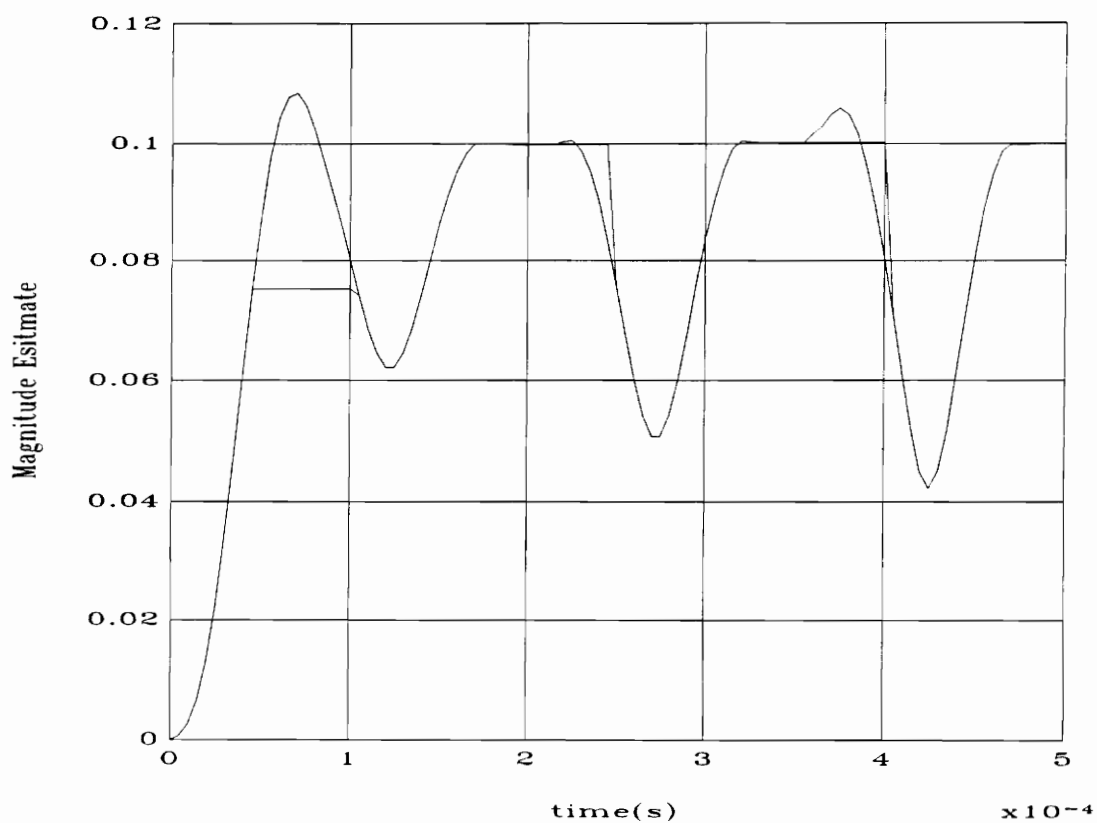


Figure 31. Magnitude estimate for a known velocity signal before and after the quality signal is applied with noise on the Doppler signals and insufficient waiting after poor quality is recognized. The flat spots in the signal after the quality signal is applied is where the quality signal goes below the threshold.

## 10. Discussion of Results

The decision to select an arctangent-type digital frequency demodulator over the zero-crossing and balanced quadricorrelator was straightforward.

Compared to the other digital frequency demodulation methods the arctangent-type has a superior SNR vs. CNR characteristic for frequency demodulation and this difference is increased when the arctangent-type phase demodulator is considered. In the laser vibrometer application a phase demodulator is just as acceptable as a frequency demodulator for most applications, so the selection of the phase demodulator is acceptable.

In addition to SNR vs. CNR, the arctangent-type demodulators require less calculation than either the zero crossing or balanced quadricorrelator demodulators. The zero-crossing method when uniform sampling is used requires interpolation to determine zero crossing locations and then a long series of decisions to determine the sign of the frequency demodulated signal. The balanced quadricorrelator requires two high-frequency differentiators as well as multiplies and a sum, and more if the magnitude of the modulated signals are not unity. If the high-frequency differentiators are approximated with first difference functions, which is likely, then the demodulators frequency-to-magnitude characteristic is not linear.

A real-time implementation of the arctangent-type demodulator to be applied to a laser vibrometer is feasible. For a He-Ne laser source and a maximum target velocity to be considered of 1 m/s, the Doppler signals must be sampled at approximately 10 MHz to allow for anti-aliasing filters. Inexpensive A/D converters

are available for this step. Assuming 8 bits of quantization then a 64K ROM lookup table may be used to perform the arctangent function in real time. Following this the phase unwrapping may occur in a second 64K lookup table or a programmable logic device. After phase unwrapping the phase demodulation is complete and the relative position signal can be decimated with a dedicated decimation chip with built-in anti-aliasing filters or the signal can be decimated without anti-aliasing by simply taking every Nth point where N is the size of the decimation. To complete the frequency demodulation a digital signal processor may be used to perform the differentiation at the lower frequency.

With the arctangent frequency demodulator applied to the laser vibrometer, specialized processing to extract only a single frequency velocity or relative position component is designed. A typical test using the laser vibrometer consists of exciting a target some known frequency and then looking at its response which, assuming linearity, is at the same frequency as the excitation. To do this a quadrature detector operating at the excitation frequency is used.

The in-phase and quadrature components generated by the quadrature detector are used to set the magnitude and phase of a local oscillator. This setup is similar to a phase-locked loop but it is not even a loop. This setup will track the velocity (relative position) signal at the excitation frequency well as long as the input CNR to the demodulator is above the critical threshold of approximately 15 dB. Since the input CNR is not known at any given point an estimate must be made. Assuming the additive noise in the vibrometer is somewhat constant, the CNR is relatively proportional to the magnitude of the Doppler signals and also the sum of the absolute values of the Doppler signals. Either of these signals, termed here

'quality' signals, may be used as an indicator of the input signal CNR or input signal quality. Assuming the quality signal is accurate the local oscillator's parameters can be slaved to the output of the quadrature detector when the input signal quality is above some predetermined threshold. Once the input signal quality goes below that threshold, the local oscillator's parameters are not adjusted by the quadrature detector until the input signal returns to acceptable quality. The low-pass filters used in the quadrature detector dictate that some number of samples with an acceptable input signal quality must be obtained before valid values are generated by the quadrature detector. The low-pass filters also determine how much noise passes through the quadrature detectors and how quickly the quadrature detector generates the local oscillator's parameters. For initial tests an all-zero low-pass filter with zeros at multiples of the excitation frequency is used. This filter causes all of the deterministic components generated by quadrature detector's mixing to be eliminated. However a better LPF for this application may exist.

## 11. Conclusion

Within this thesis several methods of digital demodulation have been reviewed with the intention of applying one of them to a laser vibrometer for real time velocity extraction. The arctangent-type demodulator was selected and then additional processing was designed to improve performance for the special case of sine-dwell tests.

The implementation of the arctangent-type frequency and phase demodulators is straightforward and most of the work in this area would involve implementation issues including automatic gain control (AGC) on the Doppler signals, wider word-widths, and real-time overflow control of the phase unwrapper. The AGC would maximize the CNR seen by the digital demodulator by making sure the full range of the A/D converters are used. If the full range is not used the A/D converters add more noise to the signal than otherwise. Wider word widths of the A/D converters also maximize the CNR seen by the demodulator. Real-time overflow control of the phase unwrapper is required in a real system. Without this feature the phase unwrap counters would overflow and erroneous results would be made.

There is much room for improvement in the low-pass filters in the quadrature detector used for the sine-dwell tests. These low-pass filters dictate the key characteristics of the demodulator including acquisition time, noise passed through, and dropout recovery. Within this thesis a simple all-zero filter was used, however this is only a simple compromise of each of the above characteristics.



In conclusion, the arctangent-type digital frequency demodulator is a simple yet effective demodulator that may be applied to a laser vibrometer that generates quadrature Doppler signals. With the specialized hardware hardware constructed to perform the phase demodulation, software may implement either a phase or frequency demodulation. The benefit of phase demodulation is its superior SNR for a given CNR. The main contributions of this thesis are the selection of the arctangent-type digital frequency and phase demodulators and the demonstration that the arctangent-type phase demodulator should be used when possible.

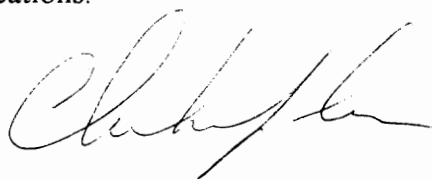
## 12. Bibliography

- 1 Drain, L.E., *The Laser Doppler Technique*, John Wiley and Sons Ltd, Chichester, 1980.
- 2 Stremmer, Ferrel G., *Introduction to Communication Systems third edition*, Addison-Wesley Publishing Company, New York, 1990.
- 3 Couch, Leon W., *Digital and Analog Communication Systems (third edition)*, Macmillan Publishing Company, New York, 1990.
- 4 Hagiwara, M., and M. Nakagawa, "Range-extended Tangent-type FM Demodulation Using Digital Signal Processing," *Electronics and Communications in Japan, Part 1*, 69, No. 7, 1986, pp. 83-92.
- 5 Boutin, N., and H. Kallel, "An Arctangent Type Wideband PM/FM Demodulator with Improved Performances," *IEEE Transactions on Circuits and Systems 1990 33rd Midwest Symposium*, vol. 1, 1990, pp. 460-463.
- 6 Zeng, X., J. Dominguez, and A. Wicks, "The Calibration of a Scanning Laser Vibrometer by a Digital FM Demodulation Technique," (unpublished) 1994.
- 7 Oka, K., and T. Mizuno and Y. Ohtsuka, "Wideband phase demodulation based on Fourier-transform techniques in optical heterodyne interferometry," *IECON'91*, pp. 1684-1689.
- 8 Jackson, L. B., *Digital Filters and Signal Processing (second edition)*, Kluwer Academic Publishers, Boston, 1989.
- 9 Oppenheim, A. V., and R. W. Schaffer, *Discrete-Time Signal Processing*, Prentice Hall, New Jersey, 1989.

## 13. Vita

Christopher J. Cronin received the B.S. and M.S. degrees in electrical engineering from Virginia Polytechnic Institute and State University, Blacksburg, VA, in 1992 and 1994 respectively.

He is currently a Member of the Technical Staff at Comsat Laboratories in Clarksburg, MD. His interests include signal processing, digital design, and communications.

A handwritten signature in black ink, appearing to read 'Chris Cronin', with a stylized flourish at the end.